CRL3 and CRL4 are functionally diverse ubiquitination complexes that regulate fundamental cell processes from human DNA damage repair to plant pathogen immunity

James Ruble

A dissertation

submitted in partial fulfillment of the

requirements for the degree of

Doctor of Philosophy

University of Washington

2017

Reading Committee:

Ning Zheng, Chair

Richard Gardner

Keiko Torii

Wenqing Xu

Program Authorized to Offer Degree:

Pharmacology

University of Washington

Abstract

CRL3 and CRL4 are functionally diverse ubiquitination complexes that regulate fundamental cell processes from human DNA damage repair to plant pathogen immunity

James Ruble

Chair of the Supervisory Committee:
Professor Ning Zheng
Pharmacology

Ubiquitination is a mechanism used by eukaryotes to precisely alter the level, functionality, and location of specific target proteins through the post-translational attachment of one or more ubiquitin tags. This attachment proceeds through a three-step enzymatic process involving ubiquitin activating proteins, conjugating proteins, and ligases. Of these three steps, the final ubiquitin ligation reaction to the target substrate shows the most variability due to the vast number of different substrates targeted by the cell. These ligase complexes are broadly divided into three families, with the Cullin-RING ligases (CRLs) comprising the largest physical structures. CRLs can be further subdivided into different complexes based on the specific Cullin backbone (1-5, 7) used to bridge the complex. Among the many roles these complexes play, CRL3 has been implicated in the oxidative stress response in animals (Nguyen et al., 2004) as well as hormone

signaling perception in plants (Lechner et al., 2011). CRL4 has been shown to be involved in a variety of cellular processes such as DNA damage repair and cell cycle regulation (Jackson and Xiong, 2009; Scrima et al., 2011). CRLs perform these functions by employing a modular architecture whereby individual substrate receptors are recruited to the complex to provide specificity for an array of possible targets.

The large variety of target substrates these complexes ubiquitinate presents the technical challenge of identifying them in the context of their individual pathways. It also points to the need for a cell to be able to precisely regulate these processes. Here we solve the crystal structure of DDB1, an adaptor component of CRL4, in complex with an N-terminal minimal binding fragment of DDA1. DDA1 has previously been shown to regulate CRL4 activity (Pick et al., 2007; Gao et al., 2017). We hypothesize this regulation is due to conformational control of the flexible BPB domain of DDB1, which normally confers a large degree of freedom to the alignment of the bound substrate with the incoming ubiquitin tag. We also show that CRL3 is involved in perception of the plant hormone salicylic acid (SA) via the hormone receptor NPR4, which binds to radiolabeled SA over a size-exclusion chromatography column. Finally, we show that NPR4 can be crystallized. We have generated a variety of monoclonal antibodies that bind to NPR4 to improve crystal packing and diffraction resolution. Taken together, these studies highlight the important role that CRLs play in eukaryotic biology as well as the importance of efficient regulatory regimes to fine-tune their activity.

TABLE OF CONTENTS

List of Figures iv

List of Tables v

List of Abbreviations vi

Chapter 1. Introduction and Background 1

Introduction 1

Ubiquitin 2

Ubiquitination and deubiquitination 3

Polyubiquitin chains 4

E1 ubiquitin activating enzymes 4

E2 ubiquitin conjugating enzymes 5

E3 ubiquitin ligases 6

Cullin-RING ligases 6

CRL4 and the DDB1 adaptor 8

DDB1 BPB domain flexibility 9

Substrate recruitment mechanisms 9

Chapter 2. DDA1 Binds to the BPB domain of DDB1 and regulates CRL4 ubiquitination 17

Abstract 17

Introduction 17

Methods 19

Protein purification 19

Data collection 19
Structure determination and refinement 19
DDA1 binding assays 20
In vitro CRL4^{Cereblon}-CK1α ubiquitination assay 20
Results 20
DDA1 residues 1-28 form the minimal binding sequence to DDB1 20
DDB1/DDA1-Nt structure determination and overview 21
Full-length DDA1 potentially makes additional contacts in the DDB1 junction region not observed with DDA1-Nt 22
Mutations of conserved DDA1-Nt residues compromise DDB1 binding 23
DDA1 does not affect CRL4^{Cereblon}-CK1α ubiquitination *in vitro* 23
Residues attaching the BPB and BPC domains proximate to bound DDA1-Nt C-terminus are flexible and conserved 24
Discussion 25
DDA1 binding to DDB1 places it in position to regulate BPB conformation 25
DDA1 regulation of CRL4 complexes is context-dependent 27
DDA1 and the *hp-1* tomato mutant: a link to plant photomorphogenesis 29
Chapter 3. NPR4 is a CRL3-based receptor for salicylic acid in plants 40
Abstract 40
Introduction 40
Methods and Materials 44
Cloning and protein purification 44
[^{3}H]SA binding assay 44

Crystallization and data collection 44
Antibody binding and Fab generation 45
Results 45
NPR4 binds salicylic acid over gel filtration 45
NPR4 crystallizes and yields low- to medium-resolution diffraction data 46
Generation of monoclonal antibodies against NPR4 47
Discussion 47
NPR4 is a salicylic acid receptor in plants 47
NPR4 can be crystallized but diffracts with poor resolution 48
Bibliography 54

LIST OF FIGURES

Figure 1.1. The ubiquitination process 12
Figure 1.2. Cullin-RING ligases 13
Figure 1.3. CRL3 and the BTB domain 14
Figure 1.4. CRL4 and the DDB1/DCAF ligase arm 15
Figure 1.5. DDB1 BPB domain flexibility 16
Figure 2.1. DDA1 N-terminal residues 1-28 are necessary and sufficient for DDB1 binding 32
Figure 2.2. DDA1-Nt binds to the BPA domain of DDB1 33
Figure 2.3. DDA1-Nt makes extended contacts flanking BPA WD40 repeat 7 34
Figure 2.4. Human DNA Damage Binding Protein 1 (DDB1) secondary structure 35
Figure 2.5. DDA1 potentially makes contacts with DDB1 not observed with DDA1-Nt 36
Figure 2.6. Mutations to conserved DDA1-Nt residues compromise DDB1 binding 37
Figure 2.7. DDA1 does not affect $CRL4^{Cereblon}$-CK1α ubiquitination *in vitro* 38
Figure 2.8. DDB1 residues connecting BPB and BPC are flexible and conserved 39
Figure 3.1. Systemic response to SA 49
Figure 3.2. NPR4 binds to [^{3}H]SA over gel filtration 50
Figure 3.3. NPR4 crystallizes and yields low- to medium-resolution diffraction data 51
Figure 3.4. NPR4 antibody binding assay 52
Figure 3.5. NPR4 binds to antibody Fab fragments 53

LIST OF TABLES

Table 2.1. Structure determination and refinement statistics 31

LIST OF ABBREVIATIONS

APC	Anaphase Promoting Complex
ADP	Adenosine Diphosphate
AMP	Adenosine Monophosphate
ATP	Adenosine Triphosphate
AUX	Auxin
BDS	Beads
BGL2	β-glucanase 2
BPA/B/C	β-Propeller A/B/C
BTB	BR-C (Broad-Complex), Ttk (tramtrack), and Bab (bric à brac)
C-Abl	mammalian Abelson murine leukemia viral oncogene homolog
CAND1	Cullin-Associated and Nedd8-Dissociated protein 1
CDD	COP10, DET1, and DDB1
Cdt1/2	Chromatin licensing and DNA replication factor 1/2
CK1α/2	Casein Kinase 1α/2
COP	Constitutive Photomorphogenesis
CRBN	Cereblon
CRL	Cullin-RING Ligase
CSA/CSB	Cockayne syndrome A/B
CSN	COP9 Signalsome
Cul	Cullin

Da	Dalton
DCAF	DDB1 and Cullin4-Associated Factor
DDA1	DET1- and DDB1-Associated 1
DDB1/2	Damaged DNA Binding protein 1/2
DDD-E2	DDB1, DET1, DDA1-E2
DET1	De-Etiolated 1
DNA	Deoxyribonucleic Acid
DTT	Dithioreitol
DUB	Deubiquitinating enzyme
EMTS	Ethylmercuric Thiosalicylate
ER	Endoplasmic Reticulum
Et	Ethyl
Fab	Antibody-binding fragment
Fgf8	Fibroblast growth factor 8
FL	Full-Length
FT	Flow-Through
FUS	Fusca (*Latin: "dark"*)
GFP	Green Fluorescent Protein
GST	Glutathione S-Transferase
HECT	Homologous to E6-AP (Associated Protein) C-terminus
HEK 293	Human Embryonic Kidney 293
HeLa	Henrietta Lacks
HIV	Human Immunodeficiency Virus

HPLC	High Performance Liquid Chromatography
IAA	Indole-3-acetic Acid
IMiD	Immunomodulatory imide Drug
JAMM	JAB1/MPN/Mov34 metalloenzyme
JAZ	Jasmonate ZIM (Zinc-finger protein expressed in Inflorescence Meristem)
Keap1	Kelch-like ECH-associated protein 1
KLHL	Kelch-Like
M	Molar
MINDY	Motif Interacting with ubiquitin-containing Novel DUB family
MJD	Machado-Joseph Disease protein domain protease
ml	milliliter
mM	millimolar
MPD	2-Methyl-2,4-pentanediol
mRNA	messenger Ribonucleic Acid
mV	millivolt
Nedd8	Neural precursor cell expressed, developmentally down-regulated 8
Neg	Negative
NF-κB	Nuclear Factor κ-light-chain-enhancer of activated B cells
NLS	Nuclear Localization Signal
nM	nanomolar
nm	nanometer
NPR1/3/4	Nonexpresser of Pathogenesis-Related Genes 1/3/4
Nrf2	NF-E2-related factor 2

NTD	N-terminal Domain
OAc	Acetoxy
OTU	Ovarian Tumor protease
PAGE	Polyacrylamide Gel Electrophoresis
PCMBS	p-Chloromercuriphenylsulfonic acid
PCNA	Proliferating Cell Nuclear Antigen
PD	Pulldown
PDB	Protein Databank
PEG	Polyethylene Glycol
PIP	PCNA-Interacting Peptide
PML	Promyelocytic Leukemia
Pos	Positive
POZ	Pox virus and Zinc finger
PR	Pathogenesis-Related
PTM	Post-Translational Modification
RBR	RING-in-Between-RING
Rbx1/2	RING box protein 1/2
RING	Really Interesting New Gene
RMSD	Root-Mean-Square Deviation
ROS	Reactive Oxygen Species
s	second(s)
SA	Salicylic Acid
SAR	Systemic Acquired Resistance

SCF	Skp Cullin F-box
SDS	Sodium Dodecyl Sulfate
SIV	Simian Immunodeficiency Virus
Skp1	S-phase kinase associated protein 1
SLBP	Stem-Loop Binding Protein
SOCS	Suppressor Of Cytokine Signaling
SUMO	Small Ubiquitin-like Modifier
SV5-V	Simian Virus 5-V
TCEP	Tris(2-carboxyethyl)phosphine
TEV	Tobacco Etch Virus
TGA	TGACGTCA cis-element-binding protein
TIR1	Transport Inhibitor Response 1
TMV	Tobacco Mosaic Virus
Tris	Tris(hydroxymethyl)aminomethane
Ub	Ubiquitin
Uba	Ubiquitin activating protein
Ubc	Ubiquitin conjugating protein
UCH	Ubiquitin C-terminal Hydrolase
Ubl	Ubiquitin ligase
UPS	Ubiquitin-Proteasome System
USP	Ubiquitin-Specific Protease
UV	Ultraviolet
WRKY	Tryptophan Arginine Lysine Tyrosine

μg	microgram
μM	micromolar

ACKNOWLEDGEMENTS

I'd like to thank my academic mentors, Rachel Powers and Ning Zheng, for their guidance and support through my scientific training. I'd also like to thank my committee members, Bill Catterall, Rich Gardner, Keiko Torii, and Wenqing Xu.

I wouldn't have been able to make it through grad school without the love and support of my wife Sim. I also want to express my sincere gratitude to her sister's family, Jas and Darrell Piche, along with their two daughters Neha and Samira. You guys have given me so much support and I couldn't have done this without you.

Chapter 1. INTRODUCTION AND BACKGROUND

INTRODUCTION

Ubiquitin is a small protein that is covalently attached to a wide array of cellular substrates to regulate virtually all major cellular processes in eukaryotes. Over the past 40 years the world of ubiquitin and ubiquitin-like proteins has been increasingly uncovered and detailed. From controlling major aspects of the cell cycle, such as cyclin stability and activity of the Anaphase Promoting Complex (APC) (Sivakumar and Gorbsky, 2015; Chang and Barford, 2014), to its role in adaptive and innate immunity (Li et al., 2016; Hu and Sun, 2016), ubiquitin is a vital and pervasive component at the center of eukaryotic biology. Improvements in our understanding of these processes have shed light on the array of ubiquitin-like proteins that exist as well as their fundamental regulatory roles throughout the cell.

Canonical ubiquitin function involves the use of post-translational attachment of poly-ubiquitin chains to a specific cellular substrate protein to target it for degradation (Hershko et al., 1980) by the 26S proteasome. Early work in the field firmly established the Ubiquitin-Proteasome System (UPS) as one of the two fundamental ways (along with the lysosome) by which a cell degrades and recycles polypeptide macromolecules (Hershko and Ciechanover, 1982; 1992). This occurs through processive, ATP-driven hydrolysis as the proteasome lid binds the polyubiquitin chain and couples the unfolding of the substrate to translocation of the nascent polypeptide through the proteasome's catalytic core (Rubin et al., 1998; Verma et al., 2002; Benaroudj et al., 2003; Smith et al., 2005, Liu et al., 2006).

The UPS gives the cell a powerful and responsive way to regulate proteostasis. Many of the proteins that comprise cell signaling pathways are short-lived, and their stability in response to

environmental events requires tight control. Interruption of constitutive degradation or degradation of otherwise stable signaling proteins are prominent mechanisms featured in many pathways, such as those regulating NF-κB and p53. Additionally, most macromolecular complexes are dynamic structures that require constant remodeling for the duration of their function. For example, the complex process of DNA replication requires successive stages of initiation, elongation, and termination that need to be precisely choreographed to ensure efficiency of the process and fidelity of the result. The UPS provides an effective way to address these requirements.

Beyond its UPS-related function, ubiquitin, and its ubiquitin-like cousins, play important roles in many other aspects of protein function. Ubiquitin-interacting domains of various types are employed to recruit mono- and polyubiquitin attachments to induce protein-protein interaction and nucleate large macromolecular complexes. For example, the Small Ubiquitin-like Modifier protein-1 (SUMO-1) is covalently attached to Promyelocytic Leukemia (PML) and other PML-binding proteins to promote formation of nuclear bodies, which are believed to regulate transcription factor dynamics (Muller et al., 1998). Furthermore, ubiquitin and ubiquitin-like protein modifications can regulate protein function directly. These examples represent a tiny fraction of the roles ubiquitin plays in fundamental cell biology.

For a comprehensive review of important aspects related to this system not covered by the scope of this dissertation, please refer to: Hochstrasser, 2009; Finley, 2009; van der Veen, 2012; Husnjak and Dikic, 2012; Geng et al., 2012; and Zheng and Shabek, 2017.

UBIQUITIN

Ubiquitin is comprised of 76 amino acid residues (Schlesinger et al., 1975; Wilkinson and Audhya, 1981) and exhibits a very stable β-grasp fold (Vijay-Kumar et al., 1985; Burroughs et al.,

2007) that is conserved among eukaryotic homologs and throughout all ubiquitin-like orthologs (figure 1.1A). In comparison, human SUMO-2 shares only 16% identity with ubiquitin, however the crystal structures of the two align within 1.5 Å RMSD (Huang et al., 2004; Vijay-Kumar et al., 1987). Sequence homology within the ubiquitin family itself is high, with 96% sequence identity shared between human and budding yeast ubiquitin orthologs. The ubiquitin C-terminus is comprised of a short, flexible tail that concludes with a di-glycine motif (Wilkinson and Audhya, 1981), a feature also shared among ubiquitin-like orthologs.

UBIQUITINATION AND DEUBIQUITINATION

The core ubiquitination process involves three steps (figure 1.1B). First, an E1 Ubiquitin activating enzyme (Uba), containing an active site cysteine residue, binds to free ubiquitin and ATP, forming a ubiquitin-AMP intermediate. Ubiquitin is then transferred to the active site cysteine. Next, the ubiquitin is transferred to a cysteine residue on an E2 Ubiquitin conjugating enzyme (Ubc). Finally, the ubiquitin Glycine-76 main chain carboxylate moiety is ligated to the epsilon amino group of the target substrate lysine by an E3 Ubiquitin ligase (Ubl), creating an isopeptide bond (Goldknopf and Busch, 1977; Hershko et al., 1980; Hershko et al., 1981).

To maintain tight regulation of ubiquitination, a cell needs to be able to reverse this process and remove post-translationally attached ubiquitin from their target substrates. Deubiquitinating enzymes (DUBs) fulfill this role. DUBs are modular proteases that are divided into six major subclasses: Ubiquitin-Specific Proteases (USPs), Ubiquitin C-terminal Hydrolases (UCHs), Machado-Joseph Disease protein domain (MJD) proteases, Ovarian Tumor (OTU) proteases, JAB1/MPN/Mov34 (JAMM) motif proteases (Nijman et al., 2005), and the newly-discovered Motif Interacting with ubiquitin-containing Novel DUB family (MINDY) proteases (Rehman et

al., 2016). USPs, UCHs, MJD proteases, OUT proteases, and MINDY proteases all use a cysteine-based catalytic triad for ubiquitin hydrolysis, while JAMMs are metalloproteases that bind zinc.

POLYUBIQUITIN CHAINS

Hershko and Heller (1985) discovered the existence of proteins with multiple ubiquitin conjugates that are covalently attached to each other. These polyubiquitin chains were not required for UPS-mediated degradation, however they greatly increased the rate of this degradation compared to monoubiquitinated conjugates. These chains were later determined to have isopeptide linkages – primarily to ubiquitin Lysine-48 for most degradation mediated by the UPS (Chau et al., 1989; Gregori et al., 1990).

Additional chain linkages have also been discovered, including Methionine-1, Lysine-6, Lysine-11, Lysine-27, Lysine-29, Lysine-33, and Lysine-63 (Komander and Rape, 2012). These linkages are employed in a variety of ubiquitination contexts in addition to the UPS. Ubiquitin contains three hydrophobic surface patches, and the alternative linkages of certain polyubiquitin chains take advantage of alternative types of packing mediated through these patches to create unique chain geometries that vary by linkage attachment type. These different types of chain geometries provide a primary means of recognition for various binding partners.

E1 UBIQUITIN ACTIVATING ENZYMES

E1 Uba enzymes bind to both ubiquitin and ATP. They catalyze the adenylation of ubiquitin (Haas et al., 1982; Haas and Rose, 1982), which is subsequently transferred to an active site cysteine residue to form a high-energy thioester bond. E1s can bind two ubiquitin molecules at a time, so that as the adenylated ubiquitin is transferred to the E1 cysteine another can begin the process in parallel. This allows the enzyme to have high catalytic efficiency: rabbit Uba1, for

example, which was purified from the original reticulocyte system (Ciehanover et al., 1978), catalyzes ubiquitin thioester formation at a rate of 1-2 s^{-1} (Haas and Rose, 1982).

Budding yeast has a single ubiquitin activating gene (Uba1), while humans have two related homologs (Uba1/Uba6). Each encodes a monomeric protein between 110 kDa and 120 kDa in weight. SUMO and Nedd8 Uba-like proteins, on the other hand, are each composed of heterodimeric structures of two separate gene products. Each complex consists of an N-terminal regulatory subunit along with a C-terminal catalytic subunit with nucleotide-binding activity (Johnson et al., 1997; Desterro et al., 1999; and Gong et al., 1999).

E2 UBIQUITIN CONJUGATING ENZYMES

E2 Ubc enzymes comprise a group of proteins that is relatively conserved from yeast to humans. They have a core domain of about 150 residues as well as divergent N- and C-termini that are involved in specific E1-E2 or E2-E3 interactions (Pickart, 2001). These termini are used to group E2s into four classes (van Wijk and Timmers, 2010). Class I E2s contain just the core domain, while class II and III enzymes have respective N- and C-terminal extensions. Class IV E2s are the largest group and contain both extensions.

Functional E2s contain an active site cysteine residue used for ubiquitin binding, which participates in a nucleophilic attack of the E1-ubiquitin complex. Unlike most proteins involved in such a mechanism, however, E2s do not have a proximate base that would normally activate the attacking cysteine residue. Instead, this function is thought to be reconstituted by the cognate E1 enzyme. Accordingly, E2s tightly bind to ubiquitin-charged E1 enzymes and ubiquitin transfer to the E2 is rapid (Haas et al., 1988), but E2s weakly bind to free E1s and free ubiquitin (Hershko et al., 1983; Miura et al., 1999).

On the other hand, unbound E2s, as well as non-functional E2s lacking the active site cysteine (UbE2E for example), preferentially bind to their cognate E3 and can display significant regulatory effects. This functionality has been observed prominently with the plant CDD (COP10-DDB1-DET1) complex (Yanagawa et al., 2004) along with the mammalian analog DDD-E2 (DET1, DDB1, DDA1, UbE2E-E2) (Pick et al., 2007). In the CDD complex, COP10 is an E2 variant that lacks the canonical active site cysteine, and the complex was initially shown to enhance E2 activity. Conversely, the DDD-E2 complex, which contains an uncharged yet catalytically active UbeE2E, inhibits ubiquitination activity *in vitro*. These two seemingly opposite E2 mechanisms are both related by a lack of ubiquitin binding, suggesting that uncharged E2s have evolved important, non-canonical functions among the cell's ubiquitination machinery.

E3 UBIQUITIN LIGASES

There are three major families of E3 ligases, defined by their conserved domains: HECT, RING, and RBR (Zheng and Shabek, 2017). All E3 enzymes operate by forming a complex with the substrate and enabling the transfer of the charged ubiquitin from the E2 cysteine to the substrate lysine residue. This discussion will focus on the Cullin-RING ligases, a subgroup of the expansive RING E3s. For a broad review of HECT and RBR ligases, please refer to Pickart, 2001; Komander and Rape, 2012; and Shabek and Zheng, 2017.

CULLIN-RING LIGASES

The Cullin-Ring-Ligases (CRLs) are a subtype of the RING family and are the physically largest members among E3s (figure 1.2A). They employ a set of Cullin homologs as an extended structural backbone onto which the RING proteins Rbx1 or Rbx2 bind the C-terminal region and the substrate receptor components bind the N-terminal region (Zheng et al., 2002). This region is

variable among CRL subtypes: the substrate arm components are specified by the N-termini of the individual Cullin homologs (including Cul1-5, 7). Like all RING E3s, CRLs operate by binding and aligning the ubiquitin-charged E2 and the substrate to induce direct ubiquitin transfer to the substrate lysine (Shabek and Zheng, 2017).

The prominent feature of the Cullin homologs is the Cullin repeat, consisting of five α-helices packed together. Three of these repeats are arranged in tandem to create a long, narrow structure that makes up the primary body of the Cullin scaffolding (Zheng et al., 2002; Angers et al., 2006; Canning et al., 2013; Muniz et al., 2013; Cardote et al., 2017). The C-terminal region of the Cullin orthologs contains a conserved lysine residue that is neddylated – a ubiquitin-like modification – to promote CRL activity (Hori et al., 1999; Liu et al., 2002; Duda et al., 2008; Rabut et al., 2011; Scott et al., 2014). This modification is part of a cycle coupled to deneddylation by the COP9 signalsome protein CSN5 and subsequent binding by the CAND1 inhibitory protein (Goldenberg et al., 2004; Fischer et al., 2011).

CRL complexes employ adaptor proteins that bridge individual substrate receptors to the Cullin N-terminus. The primary Cullin-binding scheme used by these adaptors involves the SKP1/BTB/POZ (S-phase Kinase domain associated Protein 1/Broad-complex, Tramtrack, and Brick à brack/Pox virus and Zinc finger) domain, composed of a core of six α-helices flanked by a three-stranded β-sheet (figure 1.3A). Each domain also contains a C-terminal extension that wraps onto its binding partner, which is the helical core in the case of a BTB dimer.

In CRL1/7 and CRL 2/5 complexes the adaptor containing this domain recruits the substrate receptor with F-box or BC-box/SOCS-box motifs, respectively (Lyapina et al., 1998; Kamura et al., 2000; 2001; Dias et al., 2002). CRL3 complexes, in contrast, employ substrate receptors containing BTB domains that bind directly to Cul3 and bypass the need for a separate

adaptor protein altogether (figures 1.2B, 1.3B) (Furukawa et al., 2003). Finally, CRL4 complexes use an entirely separate mechanism for substrate recruitment that does not involve the SKP1/BTB/POZ domain.

CRL4 AND THE DDB1 ADAPTOR

CRL4 complexes are a fundamental component of eukaryotic biology that is conserved from fission yeast to humans. They regulate vital cellular functions such as transcription, cell cycle progression, DNA damage repair, and chromatin remodeling (Jackson and Xiong, 2009; Iovine et al., 2011; Scrima et al., 2011; Lee and Zhou, 2012; and Sang et al., 2015). The primary components of these complexes are Cullin4 (Cul4), Rbx1 (the RING), and DDB1 (DNA-Damage Repair 1, the Cul4-bound adaptor), along with a sizeable (60+) variety of DCAF (DDB1 and Cullin4-Associated Factor) proteins used as substrate receptors (figures 1.2C, 1.4A) (Jin et al., 2006). Humans have two versions of Cul4 – Cul4A and Cul4B.

CRL4 complexes use an entirely different type of adaptor protein than other CRL complexes to anchor substrate receptors, which employ some variation of the BTB/POZ domain in their binding mechanism. The crystal structures of DDB1 (Li et al., 2006) as well as the Cul4-Rbx1-DDB1 complex (Angers et al., 2006) show that DDB1 is composed of multiple WD40 repeat domains, also known as β-propellers. These form cylindrical folds comprised of seven sets of four antiparallel β-strands organized radially around a central axis (Murzin, 1992). The β-strands are joined by loops that project away from the top and bottom faces of the ring. Many critical protein-protein interactions involve conserved residues in these loops. β-propellers form stable, robust platforms that provide essential binding surfaces for many CRL4 complexes.

DDB1 is composed of three of these domains: BPB (β-propeller B) forms a singular domain that binds to the N-terminal region of Cul4A/B (figure 1.4B). In addition to contacting

the “top” surface of the BPB domain with helices two and five of the first Cullin repeat, Cul4A/B also contain an N-terminal extension that binds to the side of BPB (Angers et al., 2006; Fischer et al., 2011). BPA and BPC form an interwoven, double-propeller fold that is shaped like a half-open clamshell and provides a rigid binding surface for DCAF substrate receptors (Li et al., 2006). The C-terminal region of DDB1 contains a helical domain that localizes to the junction region between BPB and BPA/BPC domains.

DDB1 BPB DOMAIN FLEXIBILITY

DDB1 has been extensively analyzed by crystallographic methods, and more than 30 individual PDB depositions exist containing the protein. Notably, the BPB domain has been shown to be flexibly linked to the rest of the protein; each of the known DDB1 structures has this domain in one of three different conformations relative to the immobile BPA and BPC domains. Docking analyses of the CRL4 complex with these three DDB1 conformations show that they enable a large degree of rotation of the entire CRL4 substrate arm about an axis defined by a line running “upward” from the central BPB pore and bisecting the BPA/BPC clamshell (figure 1.5). This results in a large overall movement of the DCAF protein as well as the bound substrate relative to the catalytic Rbx1/E2 side of the CRL4 complex. No known studies have directly addressed the functional implications of this movement, however, and it remains unknown what purpose it serves or whether it is regulated in any way. How this structural plasticity of DDB1 might affect certain substrates or how this movement might be regulated are yet to be discovered.

SUBSTRATE RECRUITMENT MECHANISMS

E3 ligases employ a variety of strategies to recruit substrates for ubiquitination. These can be broadly grouped into the recognition of intrinsic elements of the substrate, post-translational

substrate modifications that induce recruitment, and small molecules to bridge the substrate and the appropriate ligase complex. The intrinsic substrate elements group can be further subdivided into use of conserved protein-protein interaction domains as well as recognition of pathological protein states such as misfolding or truncation.

One of the early ubiquitination pathways to be discovered was the "N-end rule," whereby truncated proteins with internally exposed residues – proteolytically cleaved perhaps – are recognized by the ubiquitin machinery through their exposed non-methionine N-termini (Bachmair and Varshavsky, 1989). The structural factors that determine substrate selectivity for this system also include an exposed lysine for ubiquitination as well as an unstructured initiation site (Prakash et al., 2004).

Other intrinsic elements of substrates used for E3 recognition are protein-protein interaction domains, such as the PIP (PCNA-Interacting Peptide) domain of Cdt1. Cdt1 is a licensing factor in the pre-replication complex that is degraded to ensure DNA is only replicated once per cell cycle (Higa et al., 2003). This degradation is effected through binding to PCNA (Proliferating Cell Nuclear Antigen) (Arias and Walter, 2006), a molecular platform originally identified as a DNA clamp and processivity factor for DNA polymerase δ (Moldovan et al., 2007). This specialized PIP box creates a degron sequence that binds to PCNA and bridges substrate proteins to the $CRL4^{Cdt2}$ complex (Havens and Walter, 2009).

Post-translational modifications (PTMs) encompass a variety of mechanisms used for substrate recognition to E3 ligases. SLBP (Stem-Loop Binding Protein) binds to the 3' stem-loop structure of histone mRNA and regulates many aspects of their maturation (Rattray and Müller, 2012). SLBP is phosphorylated on Threonine-60 and Threonine-61 by CK2 (Casein Kinase 2) and cyclin A/Cdk1, respectively (Koseoglu et al., 2008; 2010). This double phosphorylation

activates the phosphodegron sequence for recognition by DCAF11 (Djakbarova et al., 2016) and subsequent recruitment to $CRL4^{DCAF11}$.

Finally, two notable examples have recently been uncovered that show CRL complexes can use small molecules to bridge the substrate to the substrate receptor. Tan et al. (2007) revealed the structural mechanism of auxin perception in plants by the SCF^{TIR1} complex. TIR1 binds auxin in a hydrophobic cavity and uses it as a "molecular glue" to recruit substrate AUX/IAA transcriptional repressors for ubiquitination. Similarly, the long-standing mechanism for thalidomide-based teratogenicity has recently been shown to involve the $CRL4^{Cereblon}$ complex (Ito et al., 2010; Fischer et al., 2014). The molecular and atomic details have revealed that Cereblon (CRBN) binds to thalidomide to recruit Fgf8 for ubiquitination, a fibroblast growth factor that has been implicated in limb development.

(A)

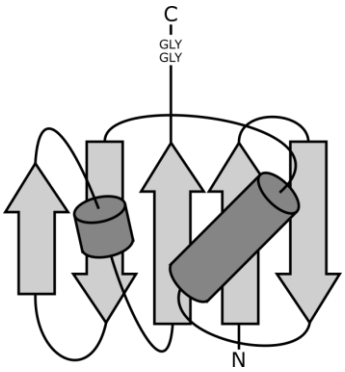

(B)

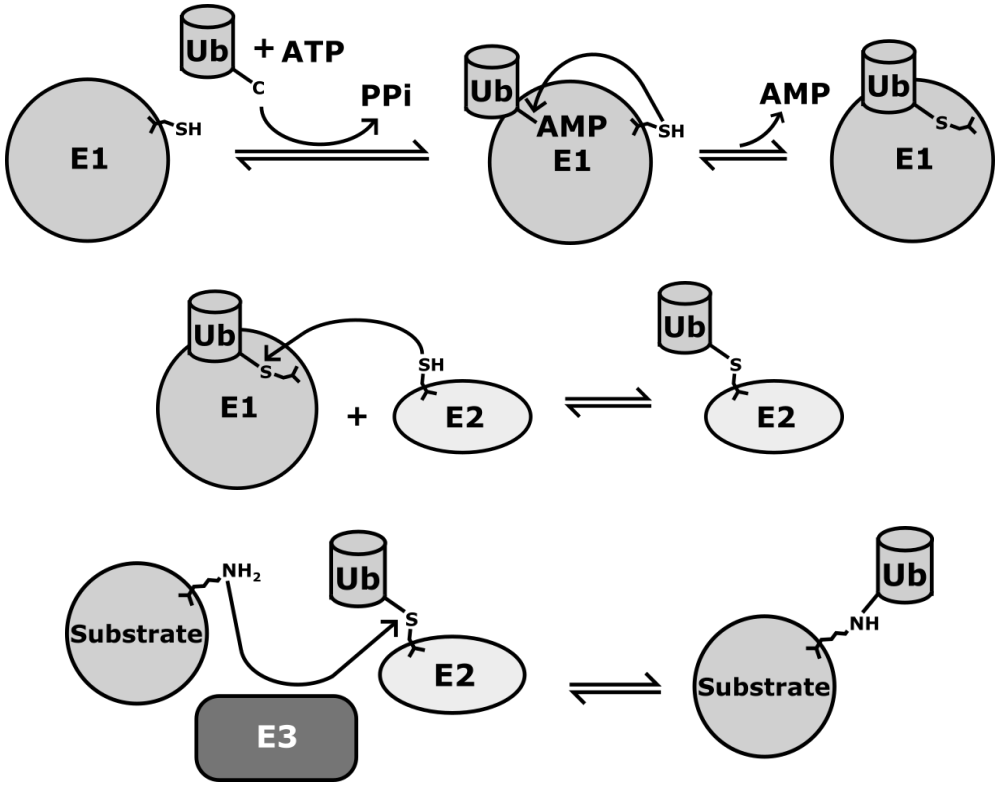

Figure 1.1. The ubiquitination process. (A) The ubiquitin secondary structure, comprising a β-grasp motif with five β-strands, two α-helices, and a C-terminal di-glycine motif. **(B)** The ubiquitination process: E1 binds to ATP-charged ubiquitin, which is then bound to the active site cysteine. The activated ubiquitin is transferred to an E2 cysteine, which is then bound to an E3 ligase to promote the transfer of the ubiquitin to the substrate lysine residue.

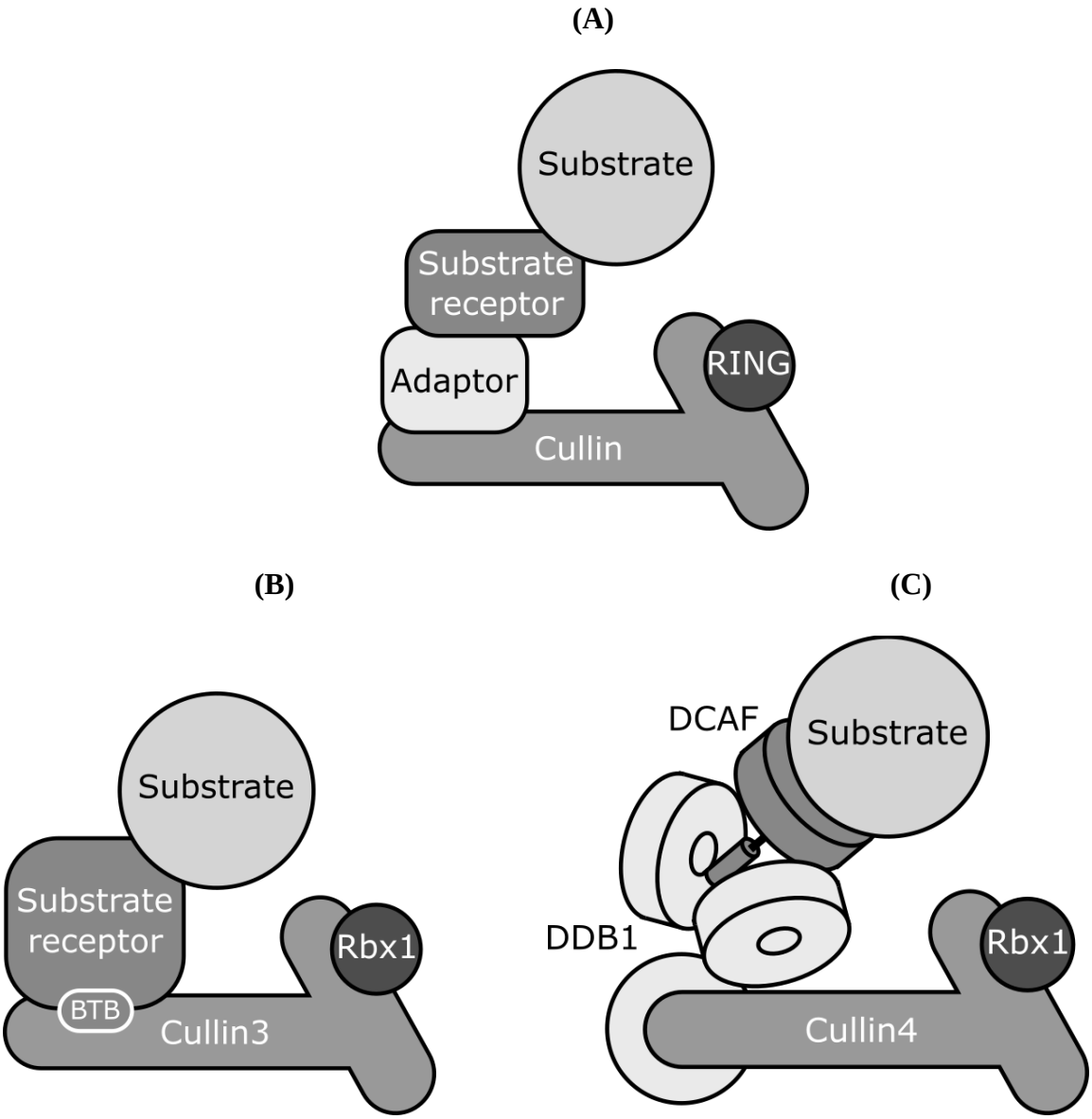

Figure 1.2. Cullin-RING ligases. **(A)** Generic CRL composition. CRL complexes employ a Cullin homolog backbone to bridge the C-terminal RING subunit to the N-terminal substrate arm, which contains the adaptor and the substrate receptor. **(B)** CRL3 combines the adaptor and substrate receptor functions into one protein, directly linking the substrate receptor to Cul3 with the conserved BTB domain. **(C)** CRL4 complexes bypass the canonical adaptor containing a SKP1/BTB/POZ domain entirely. DDB1, a large protein with three β-propeller domains, serves as the CRL4 adaptor. The BPB domain binds to the Cul4 N-terminus while the interlocked BPA and BPC domains bind to the DCAF substrate receptor.

(A)

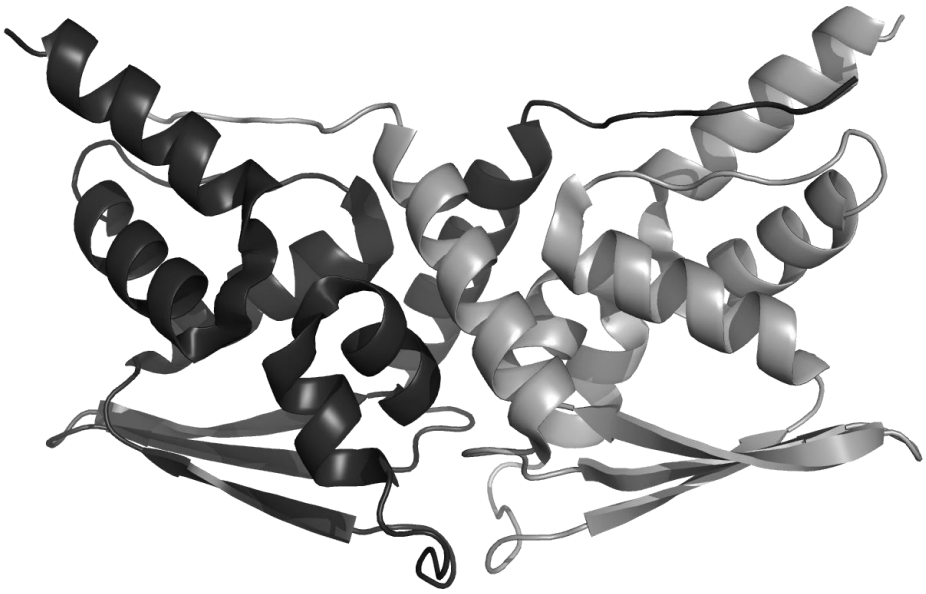

(B)

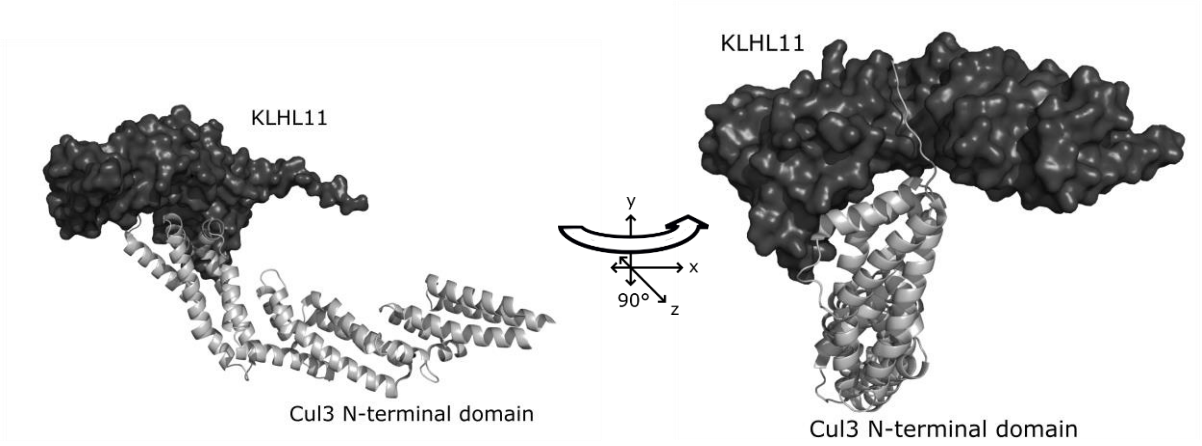

Figure 1.3. CRL3 and the BTB domain. **(A)** The Keap1 BTB domain dimer (PDB 4cxi). The BTB domain is composed of a core domain of six α-helices packed together and flanked by a three-stranded β-sheet. Each monomer also contains a C-terminal extension that projects into the side of the binding partner's core domain. **(B)** The crystal structure of Cul3 NTD (light gray) and KLHL-11 (dark gray) (PDB 4ap2).

(A)

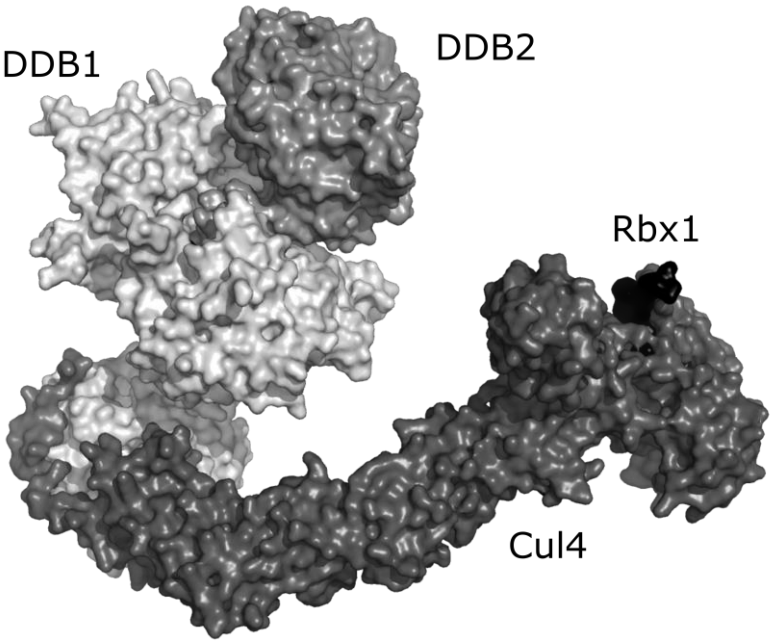

(B)

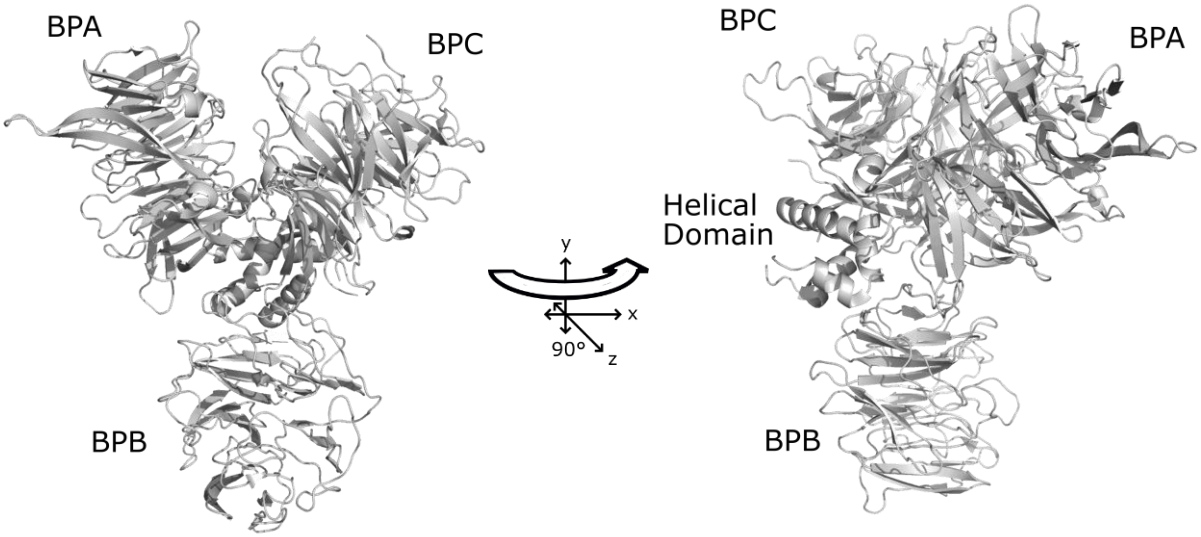

Figure 1.4. CRL4 and the DDB1/DCAF ligase arm. **(A)** The crystal structure of the CRL4 complex with DDB2 DCAF protein (PDB 4a0k). **(B)** DDB1 cartoon secondary structure showing the three β-propeller domains (BPA, BPB, BPC) and the C-terminal helical domain (right) (PDB 2b5m).

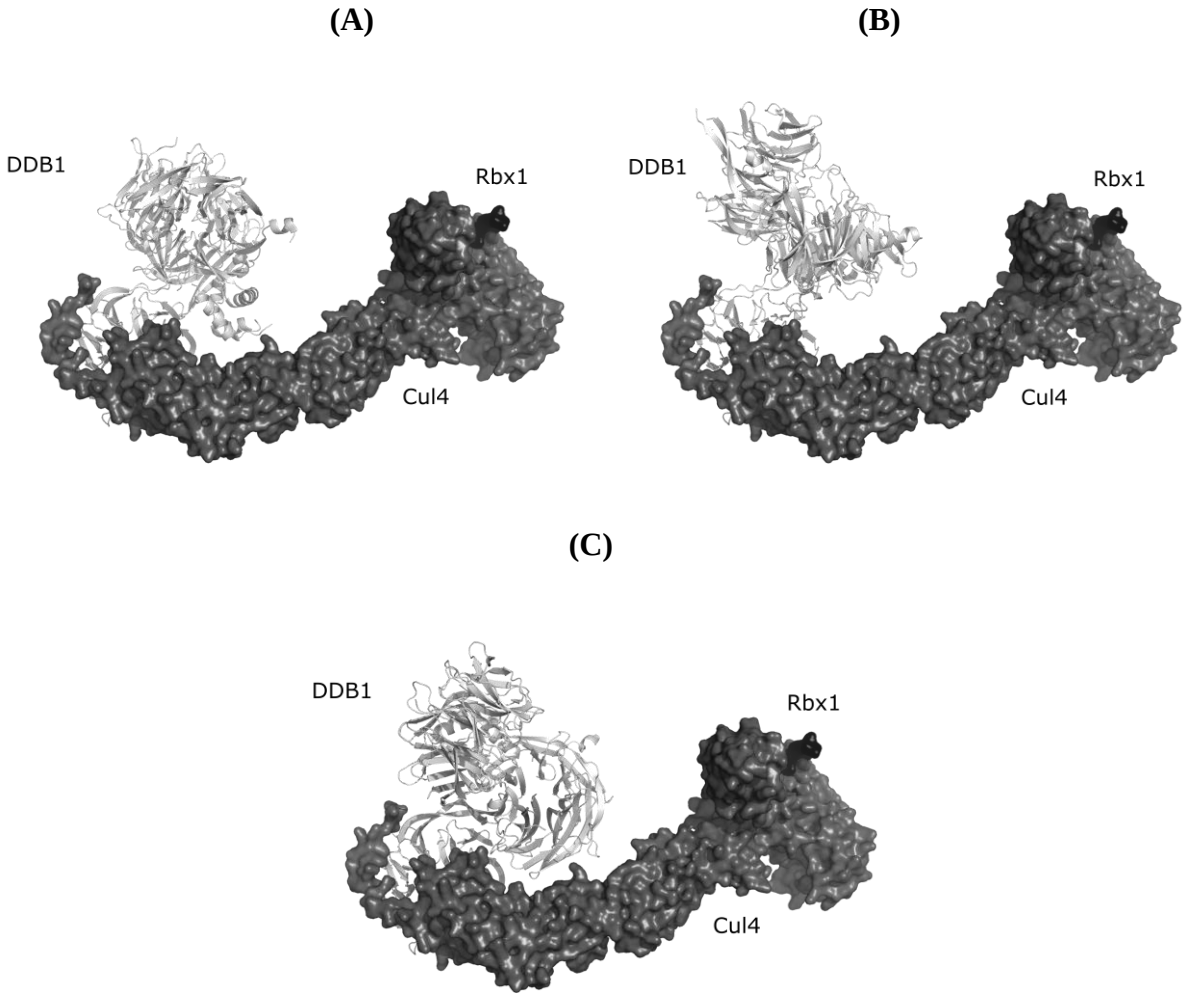

Figure 1.5. DDB1 BPB domain flexibility. Docking analyses of CRL4 with three separate DDB1 BPB domain conformations. **(A)** CRL4 (PDB 4a0k) docked to the DDB1 conformation observed in PDB 4ci1. BPA and BPC are stacked in line with a central z-axis perpendicular to the Cul4 backbone, and the C-terminal helical domain approaches Cul4. **(B)** CRL4 with DDB1 in conformation as crystallized in PDB 4a0k. BPA/BPC are stacked in line with an axis that has rotated about 90° and is roughly perpendicular to the z-axis, and the helical domain is positioned behind BPA/BPC. **(C)** CRL4 (PDB 4a0k) docked to DDB1 conformation observed in PDB 4a11. The BPA/BPC axis has rotated an additional 45° and the DCAF binding face comprised of the inner clamshell surface of BPA/BPC has pivoted downward toward Cul4 by about 45°. The helical domain has rotated superiorly and to the left, behind BPA/BPC.

Chapter 2. DDA1 BINDS TO THE BPB DOMAIN OF DDB1 AND REGULATES CRL4 UBIQUITINATION

ABSTRACT

Ubiquitination is a post-translational modification used to alter macromolecular interactions to promote protein degradation, change cellular location, and alter protein activity. Cul4-based E3 ligases ubiquitinate a variety of proteins involved in fundamental cellular processes such as transcription, DNA repair, and cell cycle regulation. DDA1 has been shown to associate with these complexes and decrease ubiquitination. Here we identify a small, N-terminal minimal binding construct of DDA1 (DDA1-Nt) that binds to the BPA domain of DDB1, the adaptor for CRL4 complexes. We observe that the C-terminal portion of DDA1-Nt protrudes into the conserved junction region connecting the flexible BPB domain, and found that full-length DDA1 likely makes additional contacts not seen with DDA1-Nt. Site-directed mutagenesis of conserved residues in DDA1-Nt do not interrupt binding, indicating distributed binding responsibility along the polypeptide. Additionally, neither DDA1 nor DDA1-Nt affect *in vitro* ubiquitination of Casein Kinase 1α, a known substrate, which, when considered with previous data on the regulatory role of DDA1 on CRL4 complexes, implies that this regulation is context-dependent. Taken together, these results suggest that DDA1 is a core functional member of CRL4 complexes and offers context-dependent regulation of their activity, possibly through the positioning of the substrate arm relative to the catalytic Rbx1-E2 portion of the complex.

INTRODUCTION

Since 2006 a few different studies have identified DDA1 (DDB1 and DET1 associated 1) as a common subunit present in certain CRL4 complexes (e.g. Olma et al., 2009). Notably, Pick

et al. (2007) identified DDA1 as part of the DDD-E2 complex (DET1, DDB1, DDA1, UbE2E-E2), which is the mammalian analog of the CDD (COP10-DDB1-DET1) complex in *A. thaliana*. This complex was discovered as part of the COP/DET/FUS loci (Chory et al., 1989; Chamovitz et al., 1996; Schroeder et al., 2002; Ma et al., 2003; Yanagawa et al., 2004), and is responsible for the repression of photomorphogenesis associated with the de-etiolation process as well as flowering (Kang et al., 2015). The mammalian DDD-E2 analog was shown to inhibit polyubiquitination *in vitro* as well as to confer Cdt1 stabilization following UV radiation in HeLa cells, indicating a broad inhibitory activity on CRL4 complexes.

An interesting study by Gao et al. (2017) established a functional role for DDA1 in the CRL4 machinery. They found that the BPA domain of DDB1 is phosphorylated by C-Abl kinase on Tyrosine-316, and this phosphorylation promotes DDA1 recruitment. DDA1 binding was shown to *potentiate* substrate degradation in cells as well as polyubiquitination in a reconstituted system *in vitro* in the presence of the immunomodulatory imide drug (IMiD) lenalidomide.

In light of the conflicting data on DDA1 function, the question remains as to how DDA1 regulates CRL4 complexes. Here we identified a short 28 residue sequence on the N-terminus of DDA1 (DDA1-Nt) that comprises the essential binding region to DDB1, corroborating previous data implicating this region (Olma et al., 2009). We solved the crystal structure of DDA1-Nt bound to DDB1 to a resolution of 3.3 Å. We determined the binding affinity of DDA1 and DDA1-Nt to DDB1, and we created site-directed mutants of conserved DDA1-Nt residues to assess their contribution to DDB1 binding. Finally, we assayed the activity of a reconstituted $CRL4^{CRBN}$-CK1α system *in vitro*.

METHODS

Protein purification

Human DDB1 was overexpressed with an N-terminal 6xHis tag in Hi5 insect cells alone as well as co-expressed with CRBN. Initial purification from cell lysate was performed by affinity chromatography with a glutathione agarose column followed by a nickel column. DDA1, DDA1-Nt, and all other DDA1 truncations and point mutants were expressed in *E. coli* with N-terminal GST tags, and initial purification was performed with a glutathione agarose column. All protein tags contained TEV protease cut sites which were used for removal. Further purification was performed with anion exchange and gel filtration columns. Final protein buffers consisted of 20 mM Tris pH 8.0, 200 mM NaCl, and 5 mM DTT.

A peptide corresponding to DDA1-Nt used for crystallography was commercially purchased and soaked into apo DDB1 crystals (Li et al., 2006). CK1α was obtained from abcam (#102102) and contained an N-terminal GST tag.

Data collection

Diffraction data was collected remotely from the Advanced Light Source at Lawrence Berkeley National Laboratory at the BL5.0.2 beamline, and indexed, integrated, and scaled with the HKL2000 software suite (Otwinoski and Minor, 1997).

Structure determination and refinement

The phase for the integrated diffraction data was solved by molecular replacement using the Phaser-MR program in the Phenix software suite v1.10.1-2155 (Adams et al., 2010) and PDB 2b5m as a source model to generate Fo-Fc and 2Fo-Fc electron density maps. An initial DDB1 model was created with AutoBuild and the DDA1-Nt polypeptide was manually fitted into the

density maps with Coot v0.8.6.1 (Emsley and Cowtan, 2004) over successive cycles of refinement in phenix.refine.

DDA1 binding assays

All assays were performed with a Pall FortéBio Octet system system. N-terminally tagged GST-DDA1, as well as all mutants and truncations, were loaded onto glutathione probes and monitored for a shift in wavelength upon incubation with DDB1. Binding affinities were calculated based on observed kinetic parameters.

In vitro CRL4^{Cereblon}-CK1α ubiquitination assay

The ubiquitination reaction contained 50 mM Tris pH 8.0, 5 mM $MgCl_2$, 2 mM DTT, 2 mM ATP, 500 μM lenalidomide, 35 μM ubiquitin, 130 nM Ube1, 2.8 μM UbcH5a, 900 nM neddylated Cul4/Rbx1, 400 nM DDB1/CRBN, 500 nM CK1α, and 1.1 μM DDA1 or DDA1-Nt. Each reaction was incubated at 37°C for 45 minutes and run on 10% NuPage Bis-Tris gels. Protein was transferred to a nitrocellulose membrane and developed with mouse anti-CK1α primary antibodies (Santa Cruz sc-74582, 1:100) and goat anti-mouse secondary antibodies (ThermoFisher #31432, 1:1000).

RESULTS

DDA1 residues 1-28 form the minimal binding sequence to DDB1

To determine the minimal DDA1 fragment for DDB1 binding we created a series of GST-tagged N-terminal and C-terminal truncations (figure 2.1A). We performed DDB1 pulldowns using glutathione agarose beads bound to the DDA1 truncation proteins (figure 2.1B). We found that the N-terminal segment of DDA1 between residues 1 and 28 is necessary and sufficient to

bind to DDB1. These results support similar findings by Jin et al. (2006) and Olma et al. (2009). We labeled this construct DDA1-Nt.

DDB1/DDA1-Nt structure determination and overview

To examine the atomic interaction of DDB1 with DDA1-Nt we crystallized the DDB1 protein in space group $P2_1$, soaked the crystals in the mother liquor containing 1 mM DDA1-Nt peptide, and solved the structure to a resolution of 3.3 Å by molecular replacement.

Briefly, the three DDB1 β-propeller domains form an upside down triangular structure (figure 2.2A; figure 2.4A). The BPB domain sits on the bottom and binds to Cul4 while the intertwined BPA and BPC domains above are arranged in a half-open, clamshell-like configuration that accommodates the DCAF receptor. The C-terminal helical domain packs against the junction point between the three domains on the Cul4-binding side of the complex. On the opposing side near this junction, DDA1-Nt forms an extended linear polypeptide that binds to the lateral and posterior surfaces of the BPA domain (figure 2.2A; figure 2.4B), while the C-terminus of DDA1-Nt projects into the deep cleft formed between the BPA and BPB domains (figure 2.2A, right).

The interface regions on the bottom surface of BPA between WD40 repeats 6-7 and 7-1 are marked by a shallow hydrophobic groove with residues that are highly conserved among metazoans (figure 2.2B). DDA1-Nt binds in this groove and creates a partition between repeat 7 and the remaining portion of the BPA domain (figure 2.3A). Most DDA1-Nt contacts are mediated by loops on the BPA domain that connect the antiparallel β-strand pairs comprising each β-propeller repeat. The contacts primarily include loops 1c, 7a, and 7c, with additional contributions from loops 1a and 6a (figure 2.4B). DDA1-Nt binding does not significantly alter the DDB1 BPB structure (figure 2.3B).

DDA1-Nt contains several conserved hydrophobic residues (figure 2.3A) that occupy surface cavities along the BPA groove. DDA1-Nt Proline-9 is invariant among all species examined and makes contacts with Valine-338 and Tyrosine-346 of loop 7c, in addition to contacts from its neighboring DDA1 residues Leucine-8 and Tyrosine-11. Phenylalanine-16 is virtually invariant (the sole exception found in the chytrid fungus *B. dendrobatidis* within all sequences examined) and projects into the central BPA cavity, contacting Leucine-29.

Phenylalanine-19 and Histidine-20 are conserved among vertebrates and occupy two additional hydrophobic patches along the BPA groove. Phenylalanine-19 sits in a pocket also contacting BPA Leucine-29 as well as Valine-44. Histidine-20 sits in a deeper pocket formed by several residues including Valine-44, Glycine-48, Leucine-49, Leucine-317, Valine-321, Leucine-333, and Methionine-350.

Another prominent contact occurs between DDA1-Nt Lysine-13 and BPA residues Arginine-270, Glycine-320, and Leucine-336. These three residues line the side of a relatively deep pocket formed at the interface of WD40 repeat 6 and 7. The DDA1-Nt backbone lies over top of this pocket and Lysine-13 projects alongside the superior margin.

Full-length DDA1 potentially makes additional contacts in the DDB1 junction region not observed with DDA1-Nt

The C-terminus of DDA1-Nt extends into the junction area between BPA and BPB domains of DDB1 and it is likely that full-length DDA1 makes additional contacts in this region. To test this idea, we immobilized GST-DDA1 and GST-DDA1-Nt on Pall FortéBio Octet glutathione probes and measured the association and dissociation of free DDB1 with the system. We found while both GST-DDA1 and GST-DDA1-Nt bound to DDB1 tightly, the dissociation constant (K_D) for the full-length protein was 28 nM while DDA1-Nt had a dissociation constant

of 663 nM (figure 2.5). These results indicate that the remaining portion of DDA1 not present in the DDA1-Nt/DDB1 crystal structure likely makes additional contacts with DDB1, and that some of these contacts probably occur near the central BPA/BPB junction region of the protein.

Mutations of conserved DDA1-Nt residues compromise DDB1 binding

DDA1-Nt makes several selective contacts along the bottom and side faces of the DDB1 BPA domain. Many of these DDA1 residues are conserved among vertebrates (Histidine-20) or among all species more generally (Proline-9, Asparagine-15, and Phenylalanine-16) (figure 2.6A). To investigate the contribution of these residues to BPA binding we created a set of mutants with these residues mutated to aspartic acid. We bound these mutants to glutathione beads with N-terminal GST tags and used them to pull down the DDB1/CRBN complex. We found that all mutants weakened the DDA1-DDB1 interactions, although none of the mutations were sufficient to completely abrogate the binding (figure 2.6B). Among these mutations, DDA1-P9D showed the weakest binding to DDB1, indicating that it plays an important role at the interface. The negative impact of the rest of the mutations to DDA1-DDB1 interaction suggests a distributed role for DDA1-Nt binding to the BPA domain that is not strictly contingent upon one or two "hot-spot" residues.

DDA1 does not affect $CRL4^{Cereblon}$-CK1α ubiquitination *in vitro*

Cereblon (CRBN) is a DCAF protein that uses the small molecule lenalidomide to recruit one of its substrates, Casein Kinase 1α (CK1α) (Ito et al., 2010; Chamberlain et al., 2014; Fischer et al., 2014). To examine the effects of DDA1 and DDA1-Nt on CRL4 function we reconstituted $CRL4^{CRBN}$-CK1α *in vitro* and observed the results on a western blot with anti-CK1α (figure 2.7). We found that neither DDA1 nor DDA1-Nt alter the amount of CK1α ubiquitination compared to

a positive control. These data suggest that either DDA1 does not regulate ubiquitination by this specific complex or that the mechanism of DDA1 regulation of this complex has not been fully recapitulated *in vitro*.

Residues attaching the BPB and BPC domains proximate to bound DDA1-Nt C-terminus are flexible and conserved

During initial DDB1 structure determination (Li et al. 2006) our lab observed limited electron density for the BPB domain when DDB1 was crystallized in the apo form. The issue was ameliorated by the addition of SV5-V as a binding partner to induce alternative crystal packing. This provided one of the first clues that the BPB domain is relatively mobile. Together with the Cul4A-DDB1 structure (Angers et al., 2006), we note a total of three different BPB orientations relative to the rigid BPA and BPC domains (i.e. PDBs 2b5l, 2b5m, and 2hye). Fischer et al. (2011) also determined multiple structures of the $CRL4A^{DDB2}$ and $CRL4B^{DDB2}$ complexes and observed the BPB domain of DDB1 in three different rotational states. Furthermore, analysis of all structural models of full-length DDB1 currently in the Protein Databank (PDB) reveals that all align to one of these three states (figure 2.8A).

Given our observation of DDA1-Nt flanking BPA WD40 repeat 7 near the central junction region (figure 2.3A, left), as well as its C-terminus projecting into the large cleft between the BPA and BPC domains (figure 2.2A, right), we reasoned that DDB1 binding by full-length DDA1 might position the protein in a manner that allows regulation of BPB rotational flexibility.

To corroborate the importance of BPB rotational movement with DDB1 function we examined the conservation of the DDB1 residues involved in this rotation among clades of species widely containing putative DDA1 homologs (figure 2.8B). Notably, among model organisms representing species from bilateral metazoans and angiosperm plants, the two flexible regions

immediately upstream and downstream from the BPB sequence show significantly more conservation than the full-length DDB1 sequence. These data reveal that BPB flexibility is of functional importance to DDB1 and suggest that DDA1 might provide structural regulation of its conformation due to its proximity.

DISCUSSION

Here we report the crystal structure of DDB1 in complex with the N-terminal fragment of DDA1 (DDA1-Nt), a short polypeptide that lacks secondary structure and adopts an extended conformation. DDA1-Nt binds to the BPA domain and makes multiple contacts with conserved residues along the BPA face opposite to the DCAF binding surface. Individual mutations to conserved DDA1-Nt residues do not completely disrupt binding, indicating a distributed role in binding affinity. Furthermore, full-length DDA1 binds to DDB1 with higher affinity than DDA1-Nt (K_D of 28 nM versus 663 nM), pointing to additional contacts likely between the DDB1 and the DDA1 C-terminal region. Finally, neither DDA1 nor DDA1-Nt affect CK1α ubiquitination as observed by a reconstituted $CRL4^{CRBN}$ assay *in vitro*.

DDA1 binding to DDB1 places it in position to regulate BPB conformation

An examination of the DDB1 secondary structure (figure 2.4) regarding the position of BPA WD40 repeat 7 is illustrative of its potential relevance to BPB conformation and the ability for DDA1 to regulate it. Downstream from BPA WD40 repeat 7 the DDB1 sequence extends back to the BPC domain and forms the first three blades of WD40 repeat 2. The sequence abruptly diverges from this repeat after the third blade, extending down into the fourth blade of BPB WD40 repeat 1. The sequence completes the entire structure of the BPB domain and projects back up

into BPC to form the final blade of the disjointed WD40 repeat 2. Finally, the sequence completes the BPC domain and ends with the C-terminal helical domain.

The juxtaposition of BPA WD40 repeat 7, BPC WD40 repeat 2, and BPB WD40 repeat 1 of the folded DDB1 protein, as well as the "splitting" of BPC WD40 repeat 2 between N-terminal and C-terminal flanks to the BPB domain, highlights their structural proximity and interconnectivity and suggests potential mechanisms whereby DDA1 binding, which surrounds the back face of BPA WD40 repeat 7, might facilitate regulation of BPB conformation. Specifically, it appears that the conformational "twisting" of the BPB domain might be structurally regulated by the relative positioning of blades 3 and 4 of BPC WD40 repeat 2 and of the loops attaching them to BPB.

We hypothesize two mechanisms to explain this regulation. First, the C-terminus of DDA1 might bind to the cleft of DDB1 between BPA and BPB in such a way as to sterically regulate BPB conformation. This seems plausible, since DDA1-Nt terminates as it approaches the bottom of the central DDB1 cleft. The presence of this cleft confers a significant degree of freedom on potential BPB movement independent of its intrinsic ability to move (figures 2.2A, 2.3B), and therefore binding in this cleft might conceivably limit or regulate this potential. Post-translational modifications to DDA1 could also play a role in this mechanism.

Second, DDA1 might induce a conformational shift in WD40 repeat 7 of the BPA domain, which would be transmitted through WD40 repeat 2 of BPC to the flexible, conserved residues that connect it to BPB. We note, however, that the lack of significant BPA conformational change with DDA1-Nt binding (figure 2.3B) reduces the prospect for this mechanism, at least without contribution from the C-terminus. Perhaps the DDA1 N-terminus simply acts as an anchor to position its C-terminus in the crucial junction region. Further structural and biochemical

characterization of DDA1 will be needed to clarify these questions. The full-length DDA1 protein in complex with DDB1 would provide valuable insight into how DDA1 accomplishes this function.

DDA1 regulation of CRL4 complexes is context-dependent

The results observed here that DDA1 does not affect $CRL4^{CRBN}$-CK1α ubiquitination *in vitro* are seemingly in conflict with some of the published results seen previously, and thus raise a fundamental question about the precise nature of the effect that DDA1 binding has on the complex. Pick et al. (2007) identified DDA1 as an intrinsic part of the DDD-E2 complex – the mammalian functional analog of the CDD complex in plants that has been shown to negatively regulate photomorphogenesis (Yanagawa et al., 2004; Kang et al., 2015). They isolated recombinant T7-Cul4A immunocomplexes from HEK 293 cells and showed that their polyubiquitination function was inhibited by recombinant DDD-E2 *in vitro*. Presumably, the heterogeneous nature of the T7-Cul4 complexes would imply that only the predominant trend on polyubiquitination function could be observed regarding regulation by the DDD-E2 complex. Any countervailing regulation on a smaller scale, or on a smaller population of substrates targeted by the variety of DCAFs represented, might be obfuscated.

Pick et al. observed little overall effect on polyubiquitination when any one of the DDD-E2 complex members were absent, including when DDA1 alone was added. In addition, they showed that the DDD-E2 complex had no effect on Cdt1 ubiquitination following exposure to UV radiation in HeLa cells. Furthermore, they found that DDA1 can bind directly to DET1 itself – apart from its association with DDB1 – and mention unpublished data showing weak polyubiquitination activity by DET1 immunocomplexes depending on the isolation condition used to obtain them. Taken together, these findings underscore the idea that DDA1 function is not

necessarily consistent across all CRL4 complexes. DDA1 displays context-dependent regulation of CRL4 function that appears to vary (or not exist) with specific DCAF and/or substrate combinations.

Gao et al. (2017) observed a positive role for DDA1 in $CRL4^{CRBN}$-IKZF1 and $CRL4^{CRBN}$-IKZF3 ubiquitination in lenalidomide-treated HEK 293T cells. This is notable in contrast to our results showing $CRL4^{CRBN}$-CK1α ubiquitination was not affected *in vitro* (figure 2.7) and highlights a situation where DDA1 seems to play different roles with the same DCAF but different substrates. This also might indicate that our *in vitro* $CRL4^{CRBN}$ ubiquitination assay showed no effect due to incomplete recapitulation of the entire system. These conflicting results underscore the idea that DDA1 function appears to be multi-faceted and context-dependent.

The differential regulatory effects of DDA1 on CRL4 in these various circumstances highlight the adaptability of CRL4 activity. Given the varying steric limitations of each potential substrate targeted by the CRL4 complex in a cell, it seems plausible that this functional flexibility of the ability of CRL4 to productively ubiquitinate these various targets is enhanced by the substantial structural flexibility of the CRL4 substrate arm. Furthermore, it seems plausible that the cell would evolve mechanisms to regulate this flexibility.

Can DDA1 regulate ubiquitination in all CRL4 complexes? Or does DDA1 provide preferential DCAF binding or substrate recruitment in specific contexts? The mammalian DDD-E2 complex highlights the functional overlap of DET1 and DDA1 (Pick et al., 2007). Olma et al. (2009) also identified a group of DDA1-DCAF complexes in HEK 293T cells. Notably, however, they did not see DET1 on this list. Future research analyzing the activity of these various complexes in the context of DDA1 binding will be needed to elucidate whether DDA1 provides

individual and context-dependent regulation of specific CRL4 complexes, or whether this regulation is of a broader character.

DDA1 and the *hp-1* tomato mutant: a link to plant photomorphogenesis

Much of the discussion thus far has been in the context of mammalian DDA1, however angiosperm plants also contain putative DDA1 homologs (figure 2.8B) with largely unknown function. The plant CDD complex was discovered to enhance the degradation of positive photomorphogenesis regulators (Yanagawa et al., 2004). Does this complex bind DDA1 like the mammalian DDD-E2 complex? One potential avenue of research suggesting this association comes from the *high pigment-1* (*hp-1*) tomato mutant, and it makes a connection between DDA1 and a potential role for its regulation of plant photomorphogenesis.

The *hp-1* tomato was originally discovered as a spontaneous mutation by the Campbell Soup Company in 1917 (Reynard, 1956) and is characterized by a deeper, richer color in the fruiting body of the plant due to an increase in lycopene production and an exaggerated phytochrome response (Peters et al., 1992). Several additional mutants were identified that phenocopied *hp-1*, including *high pigment-2* (*hp-2*) (Soressi et al., 1975). Forward genetic screening identified a *de-etiolated1* (*det1*) mutation that resulted in constitutive, light-independent de-etiolation in seedlings (Chory et al., 1989). These mutations were eventually mapped (Yen et al., 1997; Van Tuinen et al., 1997; Mustilli et al., 1999; Lieberman et al., 2004) to genes encoding DDB1 (*hp-1*) and DET1 (*hp-2*, *det1*). Notably, these two proteins have also been shown to interact in plants to regulate photomorphogenesis (Schroeder et al., 2002).

Lieberman et al., (2004) showed that the *hp-1* mutant was caused by a missense mutation to tomato DDB1 Asparagine-311, changing it to a tyrosine residue. This residue aligns to human Asparagine-319, which resides on BPA loop 7a and would contact Asparagine-15 of DDA1. To

our knowledge, no other functionality has been discovered relating to this area of the BPA domain apart from its contribution to the β-propeller structure. This provides circumstantial evidence to suggest that DDA1 might be involved in CRL4 regulation in plants, and more specifically that DDA1 might have a prominent regulatory role in photomorphogenesis.

Table 2.1. Structure determination and refinement statistics.

Crystal Properties	
Space group	p 1 21 1
a (Å)	63.196
b (Å)	219.172
c (Å)	89.317
α (°)	90.000
β (°)	89.977
γ (°)	90.000
Diffraction Data	
Resolution (Å)	3.3
Observations	189672
Unique reflections	36620
Redundancy	5.4
Completeness (%)	95.8
Overall I/σ	19.5 (1.9)
Refinement Statistics	
Resolution limits (Å)	47.8-3.3
Total atoms	17964
R_{work} (%)	23.8
R_{free} (%)	35.0

(A)

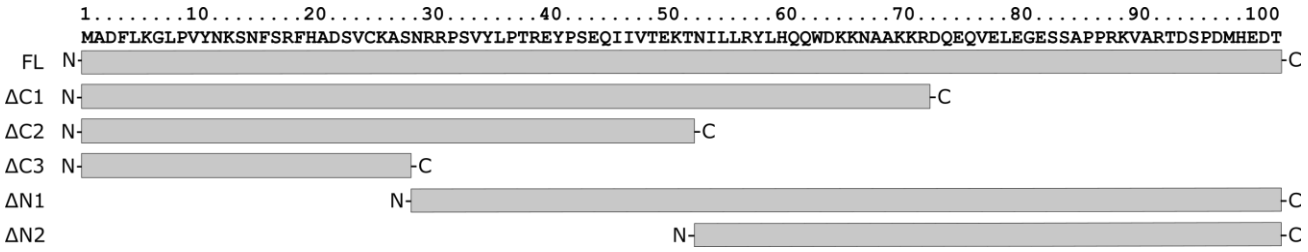

(B)

DDA1 construct:	**DDB1 binding?**
Full-length:1-102	Yes
ΔC1: 1-72	Yes
ΔC2: 1-52	Yes
ΔC3: 1-28	Yes → DDA1-Nt
ΔN1: 29-102	No
ΔN2: 53-102	No

Figure 2.1. DDA1 N-terminal residues 1-28 are necessary and sufficient for DDB1 binding. **(A)** DDA1 C-terminal (ΔC) and N-terminal (ΔN) truncation constructs were created with an N-terminal GST tag. **(B)** DDA1 truncations were isolated with glutathione agarose resin following incubation with recombinant DDB1 to assess binding ability. The minimal binding fragment, ΔC3, was selected for crystallization and named DDA1-Nt.

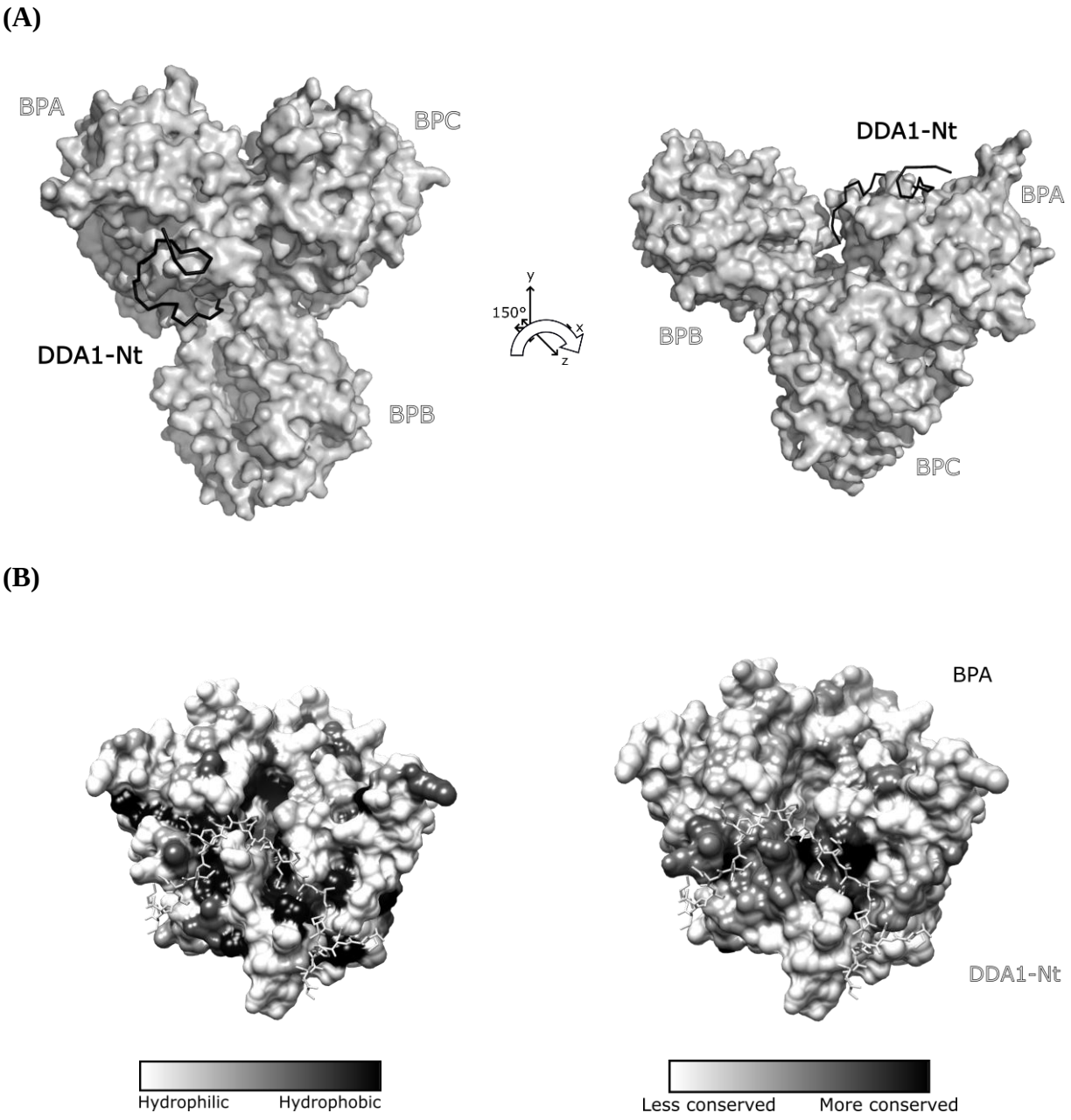

Figure 2.2. DDA1-Nt binds to the BPA domain of DDB1. (A) Surface representation of DDB1 (light gray) with DDA1-Nt in ribbon form (black) bound to the BPA domain. DDA1-Nt binds to the "back" face of BPA, opposite the side of DCAF binding (left). The DDA1-Nt C-terminus projects into the cleft between BPA and BPB (right). **(B)** DDB1 BPA domain surface representation with bound DDA1-Nt (light gray) showing hydrophobicity patches (left, black) and conserved regions among metazoans (right, black).

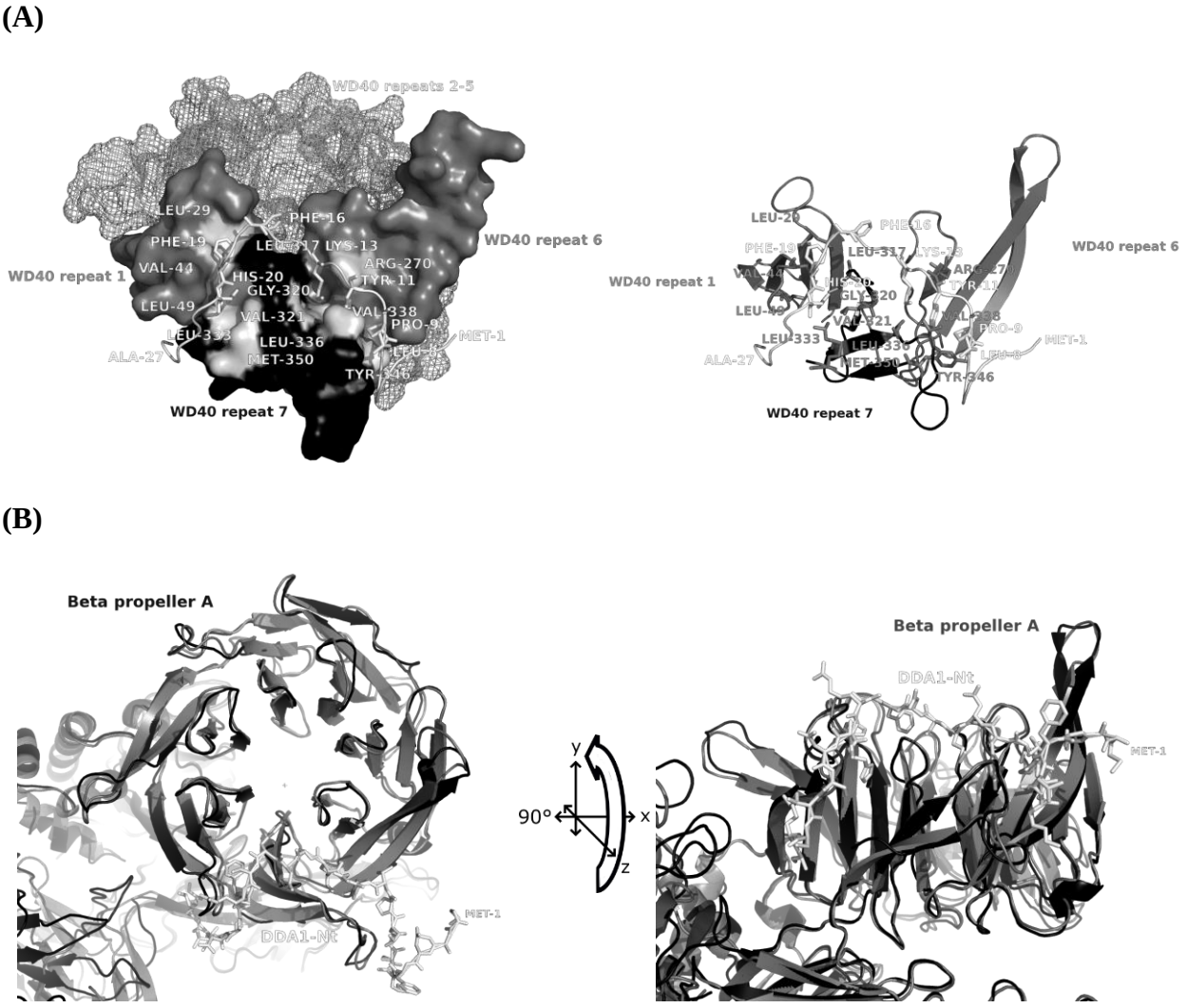

Figure 2.3. DDA1-Nt makes extended contacts flanking BPA WD40 repeat 7. (A) DDA1-Nt (white) lies along the periphery of WD40 repeat 7 (black) near the boundaries with repeat 1 and repeat 6 (gray). DDA1-Nt makes several contacts with shallow BPA pockets (light gray) along this periphery (left: BPB surface representation; right: BPB cartoon secondary structure). **(B)** DDA1-Nt binding does not significantly alter BPA structure. Overlay of DDB1 (PDB 2b5l, gray) with DDB1/DDA1-Nt (black/white).

(A)

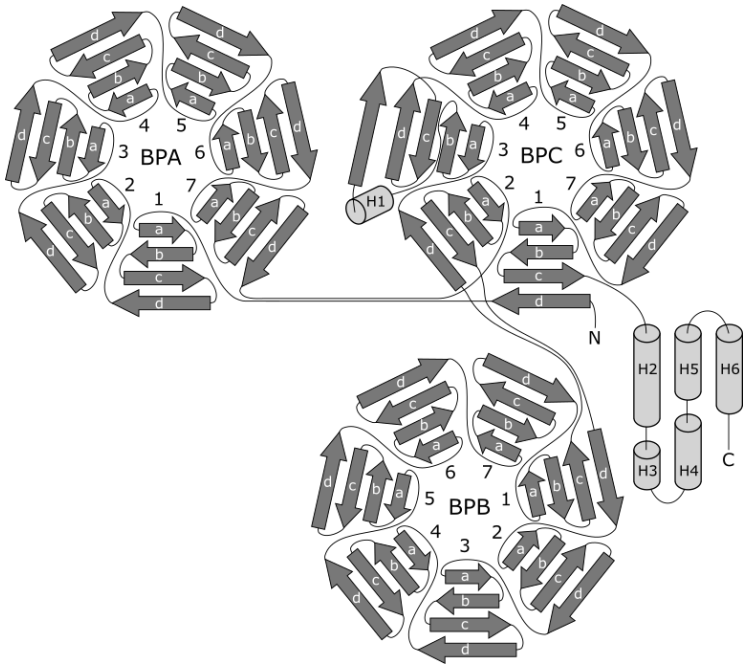

(B)

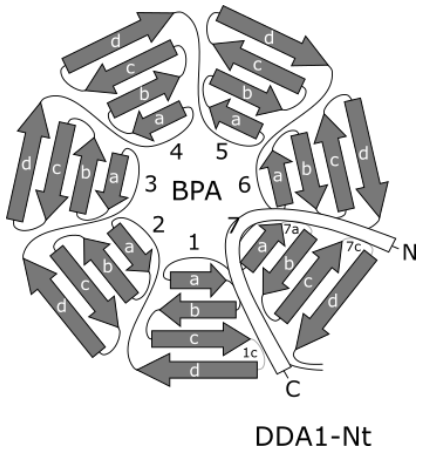

Figure 2.4. Human DNA Damage Binding Protein 1 (DDB1) secondary structure. (A) The complete DDB1 secondary structure is displayed showing BPA, BPB, and BPC, along with the C-terminal helical domain. Each β-propeller domain is composed of seven WD40 repeats arranged around a central pore. **(B)** DDA1-Nt (white) binds to the "back" face of the BPA domain – opposite to DCAF binding – and flanks WD40 repeat 7, making significant contacts with loops 1c, 7a, and 7c (gray).

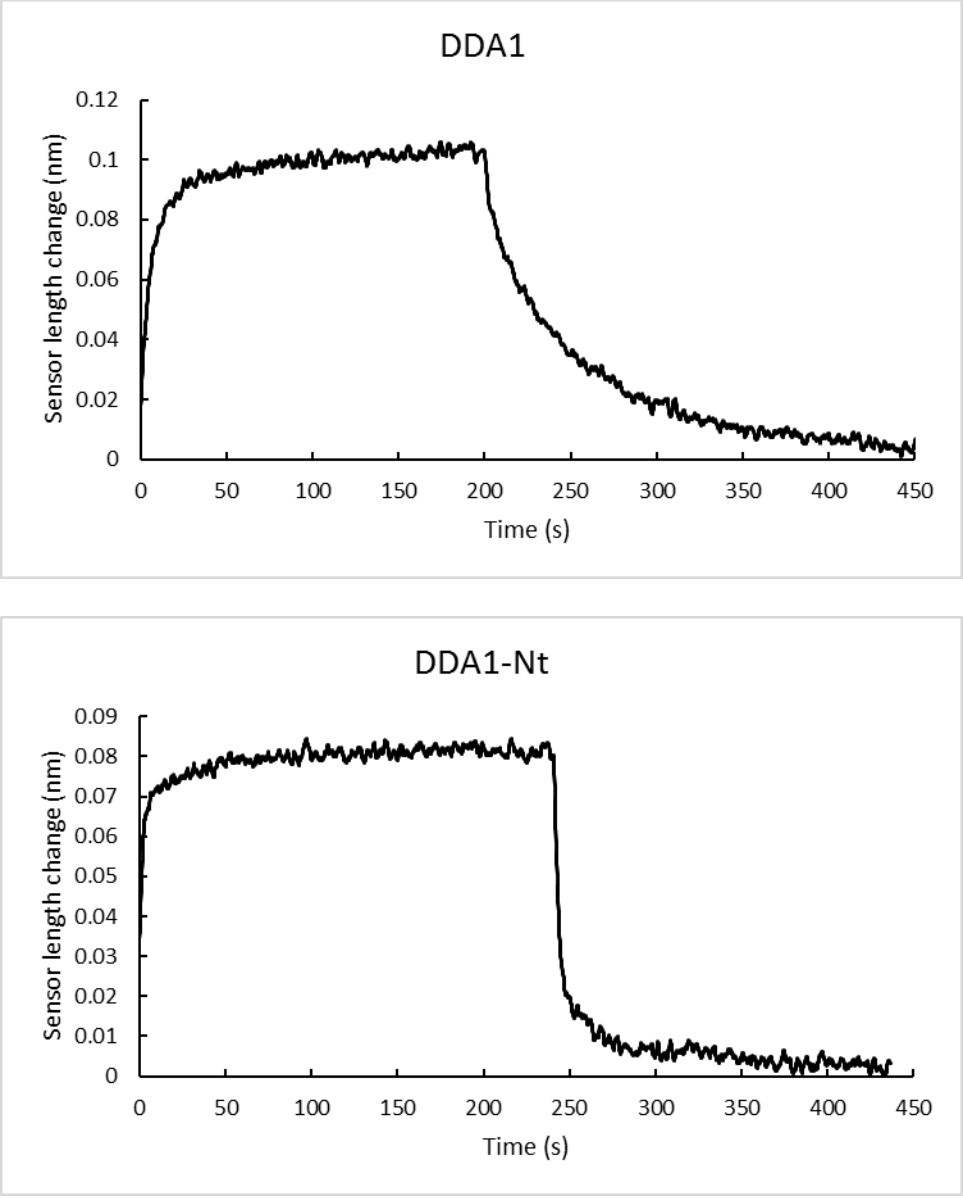

Figure 2.5. DDA1 potentially makes contacts with DDB1 not observed with DDA1-Nt. DDA1 binds to DDB1 with an affinity (K_D) of 28 nM (top), while DDA1-Nt binds with an affinity of 663 nM (bottom). The C-terminus of DDA1 might therefore make additional contacts with DDB1 not observed in DDA1-Nt.

(A)

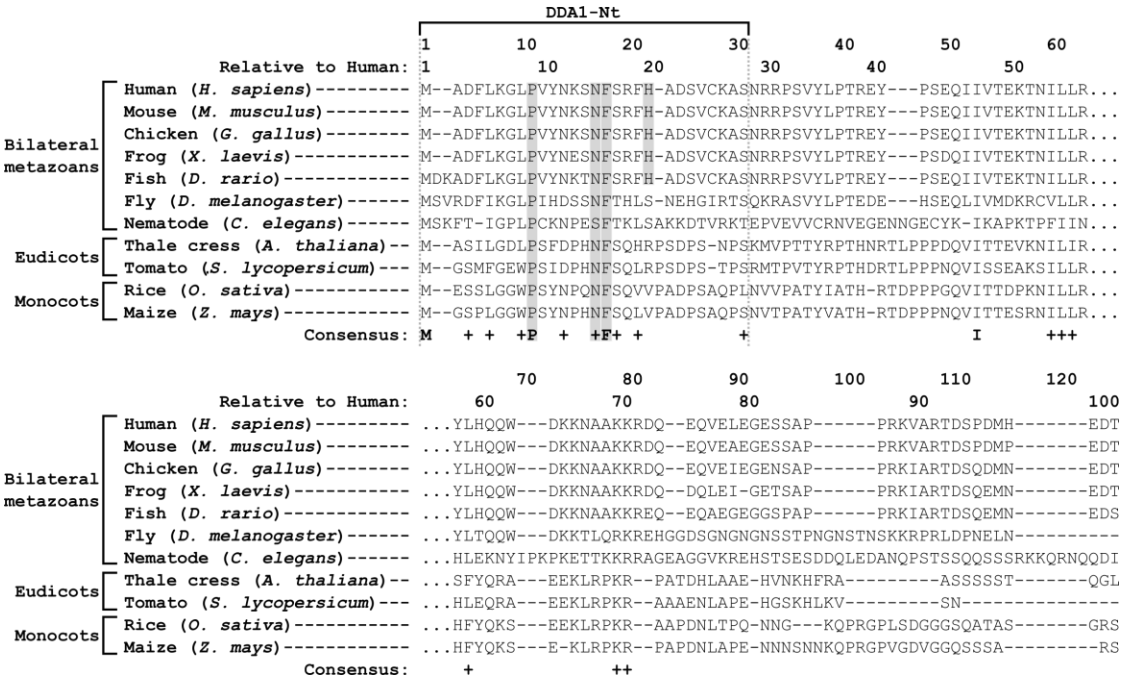

(B)

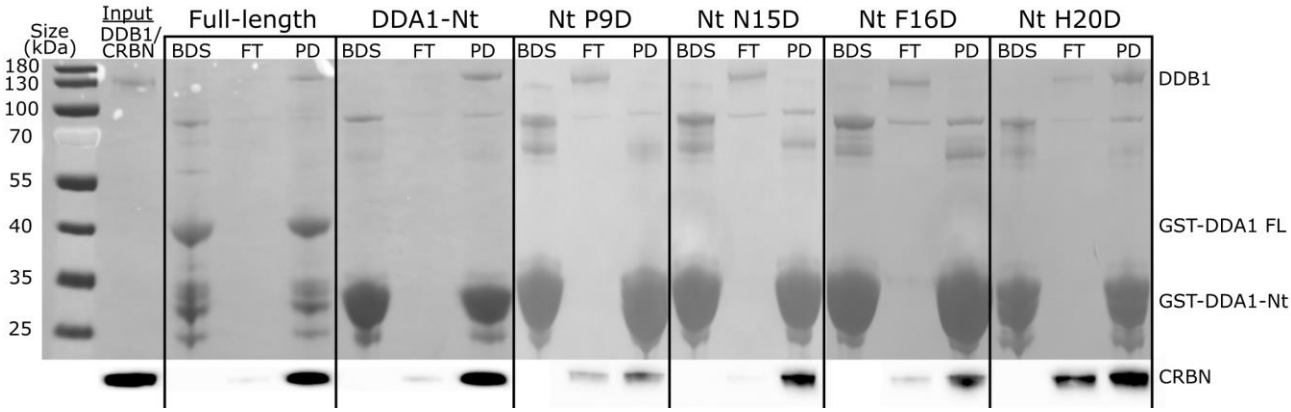

Figure 2.6. Mutations to conserved DDA1-Nt residues compromise DDB1 binding. (A) The DDA1 sequence conservation among bilateral animals and angiosperm plants is shown. Putative DDA1 homologs exist sporadically among other eukaryotes but not to the significant degree present among these groups. DDA1-Nt (residues 1-28) displays the highest region of conservation. Sites selected for DDA1-Nt binding mutations are highlighted. **(B)** Individual mutations of conserved residues Proline-9 (P9D), Asparagine-15 (N15D), Phenylalanine-16 (F16D), and Histidine-20 (H20D) reduce, but do not completely disrupt, GST-DDA1-Nt binding to DDB1/CRBN (BDS: beads; FL: full-length; FT: flow-through; PD: pulldown).

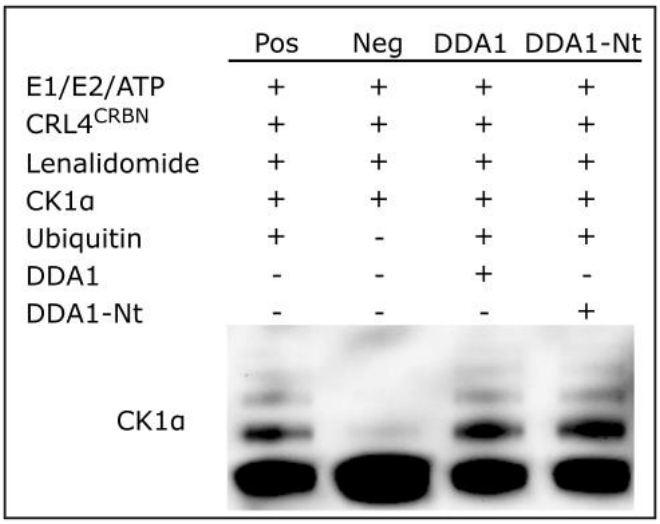

Figure 2.7. DDA1 does not affect CRL4^{Cereblon}-CK1α ubiquitination *in vitro*. CRL4^{CRBN}-mediated polyubiquitination of CK1α was reconstituted *in vitro* and used to assess DDA1 and DDA1-Nt regulation of the complex's activity. Neither DDA1 nor DDA1-Nt affect CK1α ubiquitination as detected by anti-CK1α.

(A)

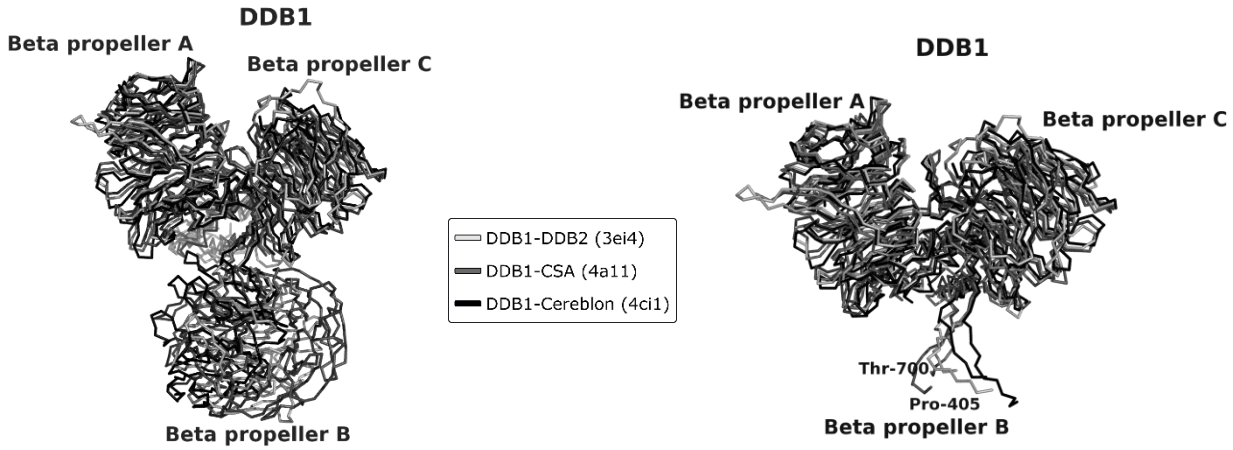

(B)

```
                    Relative to Human: 374   380       390       400       410 ...687          700       710       720
Bilateral metazoans Human (H. sapiens)---------- QLVTCSGAFKEGSLRIIRNGIGIHEHASIDLPGIKGLWPL...YPDSLALANNSTLTIGTIDEIQKLHIRTVPLYES-PRKIC
                    Mouse (M. musculus)--------- QLVTCSGAFKEGSLRIIRNGIGIHEHASIDLPGIKGLWPL...YPDSLALANNSTLTIGTIDEIQKLHIRTVPLYES-PRKIC
                    Chicken (G. gallus)--------- QLVTCSGAFKEGSLRIIRNGIGIHEHASIDLPGIKGLWPL...YPDSLALANNSTLTIGTIDEIQKLHIRTVPLYES-PRKIC
                    Frog (X. laevis)------------ QLVTCSGAFKEGSLRIIRNGIGIHEHASIDLPGIKGLWPL...YPDSLALANNSTLTIGTIDEIQKLHIRTVPLFES-PRKIC
                    Fish (D. rario)------------- QLVTCSGAFKEGSLRIIRNGIGIHEHASIDLPGIKGLWPL...YPDSLALANNSTLTIGTIDEIQKLHIRTVPLYES-PKRIC
                    Fly (D. melanogaster)------- QIITCSGSFKDGSLRIIRIGIGIQEHACIDLPGIKGMWSL...YPDSLALANKNAVILGTIDEIQKLHIRTVPLGEG-PRRIA
                    Nematode (C. elegans)------- QLVTCTGADKDGSLRVIRNGIGIDELASVDLAGVVGIFPI...YRDCLVISDGNSMVFGTVDDIQKIHVRSIPMGESVLR-IA
Eudicots            Thale cress (A. thaliana)--- QVVTCSGAFKDGSLRVVRNGIGINEQASVELQGIKGMWSL...FPDSLAIAREGELTIGTIDDIQKLHIRTIPLGEH-ARRIC
                    Tomato (S. lycopersicum)---- QVVTCSGAYKDGSLRIVRNGIGINEQASVELQGIKGMWSL...FPDSLAIAKEGELTIGTIDEIQKLHIRSIPLGEH-ARRIS
Monocots            Rice (O. sativa)------------ QVVTCSGAFKDGSLRVVRNGIGINEQASVELQGIKGLWSL...IPDSLAIAKEGELSIGTIDDIQKLHIRTIPLNEQ-ARRIC
                    Maize (Z. mays)------------- QVVTCSGAFKDGSLRVVRNGIGINEQASVELQGIKGLWSL...FPDSLAIAKEGELSIGTIDDIQKLHIRTIPLNEQ-ARRIC
                                  Consensus: Q++TC+G  K+GSLR++R GIGI E A+++L G+ G++ +...+ D+L++     + +GT+D+IQK+H+R++P+ E   + I
```

		Overall		Flexible region	
		Conserved	Similar	Conserved	Similar
Bilateral metazoans	Human (*H. sapiens*)	100%	100%	100%	100%
	Mouse (*M. musculus*)	99%	99%	100%	100%
	Chicken (*G. gallus*)	97%	98%	100%	100%
	Frog (*X. laevis*)	93%	96%	99%	100%
	Fish (*D. rario*)	91%	95%	100%	100%
	Fly (*D. melanogaster*)	61%	76%	77%	88%
	Nematode (*C. elegans*)	37%	60%	54%	82%
Eudicots	Thale cress (*A. thaliana*)	53%	69%	71%	87%
	Tomato (*S. lycopersicum*)	52%	69%	71%	87%
Monocots	Rice (*O. sativa*)	53%	69%	71%	86%
	Maize (*Z. mays*)	53%	69%	71%	87%

Figure 2.8. DDB1 residues connecting BPB and BPC are flexible and conserved. (A) The residues connecting BPB to BPC are flexible and confer a significant degree of freedom onto CRL4 ligase arm movement. These residues have been observed in three distinct conformational states among all current DDB1 crystal structures, with examples from DDB1-DDB2 (PDB 3ei4, red), DDB1-CSA (PDB 4a11, green), and DDB1-CRBN (PDB 4ci1, blue) presented. Left: BPA and BPC domains are aligned to show BPB conformational freedom. Right: The BPB domain is truncated to show flexible inbound (Proline-405-) and outbound (Threonine-700+) residues. **(B)** The flexible DDB1 residues connecting BPB to BPC are significantly more conserved than the overall DDB1 sequence among bilateral metazoans and angiosperms.

Chapter 3. NPR4 IS A CRL3-BASED RECEPTOR FOR SALICYLIC ACID IN PLANTS

ABSTRACT

Plants have evolved a variety of interconnected biochemical systems for combating pathogen infection. Systemic acquired resistance allows a plant to upregulate systemic defensive transcriptional programs in response to a localized infection. This signal is carried by the locally synthesized hormone salicylic acid, which diffuses systemically to effect its signal and is perceived by NPR3 and NPR4 (Fu et a., 2012). These proteins contain BTB domains and act as CRL3 adaptors. Here we confirm that NPR4 binds to salicylic acid *in vitro*. We also show that NPR4 can be crystallized and provides low- to medium-resolution diffraction data. Finally, we generated monoclonal antibodies to induce alternative NPR4 crystal packing conformations. The structural details of the salicylic acid perception mechanism by NPR3 and NPR4 is vital to understanding the nature of plant immune response to pathogens as well as to more generally illuminate the atomic details of CRL3 substrate recruitment.

INTRODUCTION

Systemic acquired resistance (SAR) represents one branch of inducible immune responses used by plants to counter pathogen challenge. Primary exposure to necrosis from a variety of pathogens initiates a hypersensitive response that sensitizes the plant to subsequent challenge (Ross, 1961). After initial pathogen exposure, localized activation of the isochorismate synthesis pathway increases levels of the hormone salicylic acid (SA), which then diffuses systemically to initiate transcription of a wide array of pathogenesis-related (PR) genes (Uknes et al., 1992). This

transcriptional response includes genes for secreted antimicrobial proteins and biosynthetic pathways for reactive oxygen species (ROS), as well as stress-related genes such as those involved in the secretory pathway and ER quality control (Wang et al., 2005). This transcriptional response is also extremely robust. In *A. thaliana*, it comprises up to 10% of the entire genome (Wang et al., 2006).

SAR was first systematically characterized by A. Frank Ross over half a century ago (Ross, 1961) and has been a major field of research since the 1980s. In his initial experiments Ross observed upon pathogen challenge of *N. tabacum* with tobacco mosaic virus (TMV) that in addition to the leaves developing characteristic circular necrotic lesions at points of infection, a well-known phenomenon at the time, the non-challenged leaves from the opposite side of the plant were subsequently resistant to infection. This resistance was sustained; it was observed initially after the second day, maximally after 7-10 days, and continued to persist past 20 days. Interestingly, the resistance was displayed against not only the TMV used to elicit the response, but also turnip mosaic virus and tobacco and tomato ringspot viruses.

For the past two decades our collaborator Xinnian Dong has undertaken a thorough genetic dissection of SAR. This work began with her development of a SAR reporter system based on the *BGL2* promoter – a characteristic PR gene transcribed during SAR (Uknes et al., 1992) that has become an established proxy for SAR activation. Using this system her group identified a mutant containing a lesion in the *npr1* (*non-expressor of pathogenesis-related genes1*) locus through a forward genetic screen that displayed insensitivity to SAR activation (Cao et al., 1994), and later enhanced pathogen resistance upon overexpression (Cao et al., 1998).

NPR1 contains an ankyrin repeat domain (Cao et al., 1997) that was later shown to mediate protein-protein interactions with the TGA class of transcription factors (Zhang et al., 1999).

Additionally, nuclear translocation of NPR1 is required for PR gene expression during SAR (Kinkema et al., 2000). NPR1 also contains a BTB/POZ domain, which is a common motif used in Cul3 binding.

More recently NPR1 has been shown to reside in the cytoplasm and form intermolecular disulfide bonds to other copies of itself in the non-induced state (Mou et al., 2003). During SAR induction NPR1 is reduced to its monomeric form, which presumably exposes a C-terminal nuclear localization sequence to allow nuclear translocation. Blocking this reduction precludes PR gene expression while site-directed mutations to disulfide-binding cysteine residues show constitutive SAR expression. Building on this mechanism, the group later showed that NPR1 monomers are continuously degraded in the nucleus in the non-induced state presumably to dampen PR expression (Spoel et al, 2009). Upon SAR induction, Serine-11 and Serine-15 are phosphorylated and NPR1 is degraded in a Cul3-dependent manner. This Cul3-mediated NPR1 degradation is required for full SAR induction and sustained PR gene transcription.

While NPR1 has recently been proposed as the long-sought receptor for SA (Wu et al., 2012), our collaborators were unable to detect direct SA binding (data unpublished). Instead, we have proposed that *A. thaliana* paralogs NPR3 and NPR4 perform the role of SA receptors by acting as adaptors to bridge NPR1 to Cul3 in the E3 ligase complex (Fu et al., 2012). SA would therefore represent the first known naturally occurring compound that functions by direct binding and regulation of several related BTB-domain proteins.

Our working hypothesis for SA perception is illustrated in figure 3.1. In the basal state, NPR1 is transcribed by WRKY transcription factors and exists in a disulfide-bound, polymeric form in the cytoplasm. Upon systemic SA influx NPR1 is reduced to its monomeric form and shuttled to the nucleus where it is phosphorylated, binds to TGA transcription factors to induce

SAR transcription, and is subsequently degraded in a Cul3-based E3 ligase complex using NPR3 and NPR4 as adaptors. This massive cycling of nuclear translocation, transcriptional activation, and importantly, Cul3-mediated degradation, is critical for sustained SAR (Spoel et al., 2009).

The structural mechanism for SA perception by NPR3/4 has not yet been established. An allosteric model might be hypothesized, however recent structural evidence from the auxin (Tan et al., 2007) and jasmonate (Sheard et al., 2010) hormone receptors suggest that a novel "molecular glue" mechanism might also be employed. This is exemplified in the case of the auxin receptor TIR1, where auxin binding creates a hydrophobic core in the central pocket of TIR1 that stabilizes binding of the degron motif of the soon-to-be-degraded transcriptional repressor. Regardless of the specific mechanism, a high-resolution crystal structure of this complex will undoubtedly shed light on this important issue in the field.

The question of how plants are able to upregulate systemic defenses in response to localized pathogen attack has been around at least as long as Ross' first experiments have posed the question. While the perception of most other plant hormones has been characterized at the atomic level, the corresponding mechanism employed to recognize SA has eluded us for over 50 years. Looking ahead to increased worldwide pressures on food production, knowledge of this aspect of plant immunity will undoubtedly prove to be essential.

Furthermore, the human genome contains more than 200 genes with predicted BTB domains (Pintard et al., 2004). In particular, the Cul3-based ubiquitin E3 ligase complex is known to be involved in the antioxidant response in human cells, where the constitutive degradation of the BTB-containing Nrf2 (NF-E2-related factor 2) transcription factor is mediated by the BTB adaptor protein Keap1 (Kelch-like ECH-associated protein 1) under basal conditions (Nguyen et al., 2004). Interestingly, like the proposed NPR1-NPR3/4 system, the Nrf2-Keap1 complex

functions as a redox sensor whose activity is modulated by cysteine residues in or around the BTB domain (Rachakonda et al., 2008). This system is involved in wide-ranging pathologies such as cancer and neurodegeneration, as well as cardiovascular, metabolic, and inflammatory diseases in humans (Magesh et al., 2012). Therefore, the pharmacological characterization of Cul3-based E3 ligase complexes is of great importance to human health as well as that of plants.

METHODS AND MATERIALS

Cloning and protein purification

All genes were cloned into a vector under T7 promoter control with an N-terminal, TEV-cleavable GST tag. These constructs were expressed in *E. coli* and initially purified from the cleared lysate with a glutathione agarose affinity column. Following elution and GST cleavage the proteins were further purified on anion exchange and gel filtration columns and eluted into a final buffer containing 0.1 M Tris pH 8.0, 200 mM NaCl, and 1 mM TCEP.

[^{3}H]SA binding assay

Full-length NPR4 was mixed with 10 μM [^{3}H]SA and incubated on ice for 1 hour. The sample was run over a Superdex 200 gel filtration column with a buffer containing 0.1 M Tris pH 8.0, 200 mM NaCl, and 5 mM DTT. The elution was collected into 0.4 ml fractions and a UV elution spectra at A280 was recorded. The fractions were assayed for radioactivity using a Perkin Elmer Tri-Carb 2810 TR Liquid Scintillator Analyzer.

Crystallization and data collection

NPR4 protein was initially screened with a 96-well hanging-drop setup using commercial libraries. Prospective hits were scaled to large hanging-drops for optimization and an ideal

condition composed of 0.1 M Tris pH 7.8, 0.3 M sodium formate, 0.1 M ammonium sulfate, 4% PEG 8000, and 2% poly-γ glutamic acid was identified. Crystals were harvested and soaked in 30-40% glycerol or MPD as a cryoprotectant, flash frozen in liquid nitrogen, and shipped to the Berkeley Advanced Light Source for data collection on beamlines BL8.2.1 and BL8.2.2. Data sets were collected, scaled, indexed, and integrated with HKL2000 (Otwinoski and Minor, 1997) and processed with the Phenix software suite v1.10.1-2155 (Adams et al., 2010).

Antibody binding and Fab generation

A sample of NPR4 1-552 was sent to the Vaccine and Gene Therapy Institute at Oregon Health and Science University and used to generate monoclonal mouse antibodies. A panel of hybridoma lines were returned, which we assayed to verify NPR4 binding over gel filtration. Briefly, GFP-NPR4 protein was mixed with each sample at varying ratios (1:40, 1:10, and 1:1) and run over a gel filtration column on a Shimadzu HPLC system. The elution was excited at 488 nm and GFP emissions at 509 nm were recorded. Antibody fragments were generated from a commercial kit and reverified for NPR4 binding as previously described.

RESULTS

NPR4 binds salicylic acid over gel filtration

To test the ability of NPR4 to bind to salicylic acid we ran purified NPR4 mixed with 10 μM [^{3}H]SA over a gel filtration column (figure 3.2) along with several sizing standards. We observed the A_{280} elution spectra and compared it to radioactivity counts from the elution fractions. We found that NPR4 eluted at the same position as the [^{3}H]SA peak, indicating NPR4 binding to SA.

NPR4 crystallizes and yields low- to medium-resolution diffraction data

To solve the atomic structure of NPR4 we purified the protein and screened it against a library of crystallization conditions. We observed that the full-length NPR4 protein readily crystallizes under multiple conditions (figure 3.3A). We also observed that these crystals yielded only low-resolution data on the order of 10-12 Å (figure 3.3B).

To resolve this issue, we noted that 22 C-terminal NPR4 residues are predicted to be unstructured, so we created an NPR4 1-552 construct to improve crystal packing. This protein also readily crystallized and showed an improvement in diffraction resolution to 8-10 Å. Finally, we created an NPR4 1-390 construct that crystallized and yielded medium-resolution diffraction data to about 3.2 Å. We collected multiple native data sets from these crystals.

To solve the phase for these data we employed three different strategies. First, we attempted to perform molecular replacement using known BTB domain and ankyrin repeat domain structures, however this approach was unable to produce coherent density maps. Next, we attempted to prepare selenomethionine-labeled NPR4 1-390 protein, however the expression yielded a low amount of protein that showed heterogeneous peaks during elution from an anion exchange column, and the resulting purified protein did not crystallize. Finally, we a screened for heavy atoms that derivatize NPR4 1-390 (figure 3.3C) and found that K_2PtBr_6 displayed a band-shift on native PAGE, indicative of derivatization. An anomalous data set was collected, however there appeared to be insufficient platinum occupancy to solve the phase. We also noted a probable zinc finger motif in the N-terminus of NPR4 and collected a zinc anomalous data set with native crystals, however this approach revealed insufficient zinc occupancy as well.

Generation of monoclonal antibodies against NPR4

To induce alternative forms of crystal packing we created a line of monoclonal antibodies against NPR4 1-552 and validated NPR4 binding using a construct N-terminally fused to GFP (figure 3.3). We combined this with each antibody in a 1:40 ratio and ran the samples over a gel filtration column to assay for a shift in the GFP emission signal of the elution spectra at 507 nm, indicative of NPR4 binding (figure 3.4).

From the pool of antibodies that displayed a shift in this peak, we chose four for further analysis (2G12, 11D8, 13D5, and 15C2). These were cleaved into their constituent antigen-binding fragments (Fab) and rerun to verify NPR4 binding. We observed that 2G12, 13D5, and 15C2 Fabs retained their ability to bind to NPR4 (figure 3.5, left). We increased the ratio of the 11D8 Fab to NPR4 to 1:10 and 1:1 and reran these samples over gel filtration. Neither of these increased-ratio samples were observed to bind to NPR4 (figure 3.5, right).

DISCUSSION

NPR4 is a salicylic acid receptor in plants

Here we observed that NPR4 binds [^{3}H]SA over gel filtration. These data bolster other studies performed by our collaborators showing that both NPR3 and NPR4 mediate NPR1 degradation *in vitro*, and that SA regulates the interaction between these proteins (Fu et al., 2012). They also show that *npr34* double mutants are defective in SAR *in vivo*.

Wu et al. (2012) reported that NPR1 binds to SA *in vitro* using an equilibrium dialysis assay where [^{14}C]SA binding was measured. SA binding required a copper ion to bridge SA to Cysteine-521 and Cysteine-529. Our collaborators were not able to detect NPR1 binding to SA, however it is possible that lack of free copper ions in the assay might have impeded this detection.

In light of these findings, the structural details of NPR3 and NPR4 bound to SA will be important to resolve the long-standing questions underlying SA perception in plants.

NPR4 can be crystallized but diffracts with poor resolution

To attempt to solve its crystal structure, we determined that full-length NPR4 can be crystallized and diffracts to about 10 Å. This resolution can be improved to around 3.2 Å when truncated to the first 390 residues, however this fragment was determined to be unable to bind SA over gel a filtration column (data unpublished). This points to the C-terminal portion of NPR4 being necessary for SA binding. It also shows that inclusion of the C-terminus in crystallization precludes sufficient diffraction resolution to solve its structure. These observations suggest the C-terminal SA binding region is either flexible or dynamic, however these properties seem to prevent a straightforward structural analysis of the region.

To address this issue, several avenues may be possible. First, NPR4 binding partners such as Cul3 or specific antibodies may be co-crystallized to improve crystal packing and limit movement of the dynamic C-terminal region. To this end, we have generated a variety of monoclonal antibodies that bind to NPR4 (figures 3.4, 3.5). Second, NPR4 orthologs may offer greater amenability to crystallization and high-resolution diffraction. Finally, NMR might be a useful tool to unlock the dynamic aspects of the C-terminus at the structural level. Despite these technical issues, however, obtaining structural data of NPR4 and its binding to SA is of great importance to both plant and animal biology, and will shed light on the critical role played by CRL3 complexes.

(A)

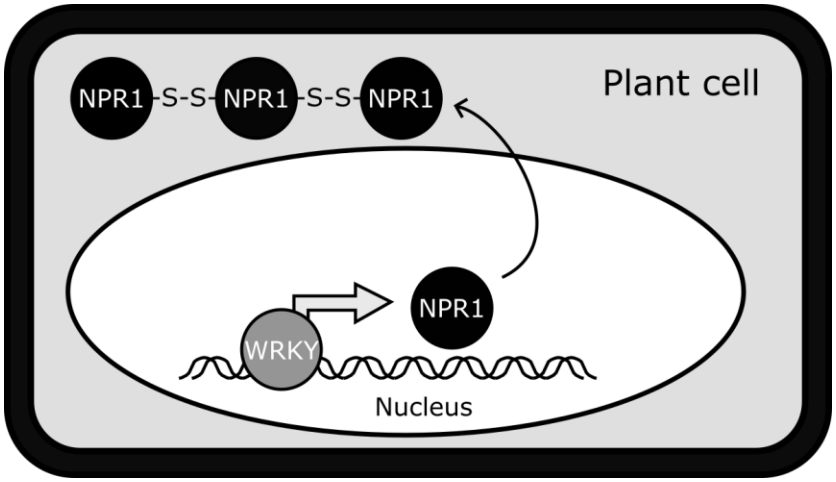

(B)

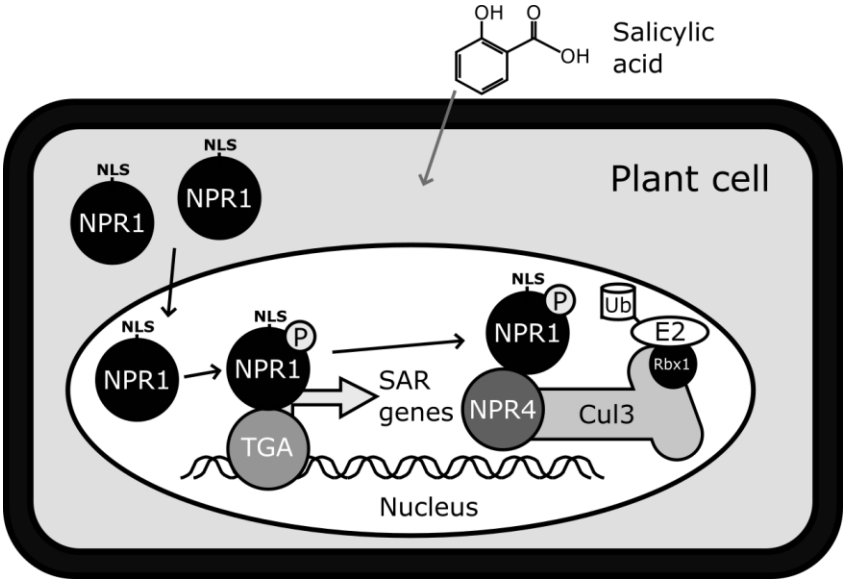

Figure 3.1. Systemic response to SA. **(A)** In the basal state without SA, WRKY transcription factors promote transcription of NPR1, which exists in an oxidized, disulfide-bound polymeric state in the cytoplasm. **(B)** Upon SA influx, these redox-sensitive disulfide bonds are reduced and NPR1 is shuttled to the nucleus where it is phosphorylated and binds to TGA transcription factors to initiate PR gene transcription. NPR1 is subsequently recruited to a Cul3-based ubiquitin ligase complex and degraded, which sustains the NPR1 cycling process and SAR.

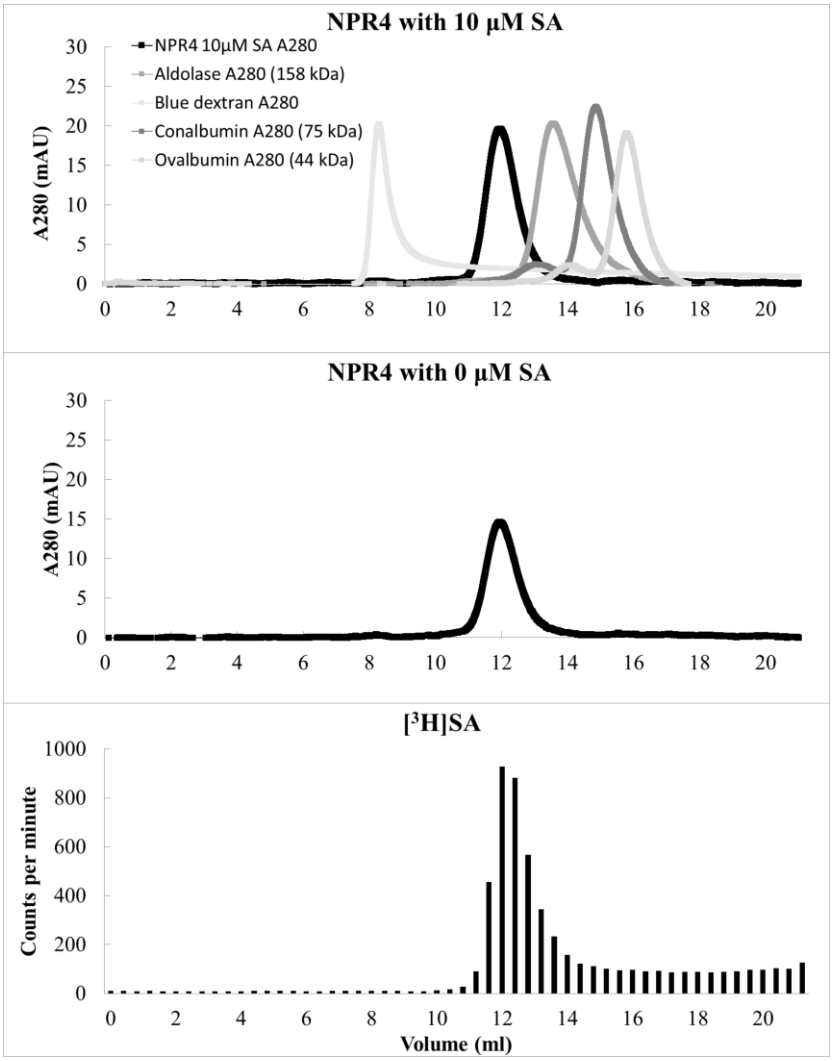

Figure 3.2. NPR4 binds to [^{3}H]SA over gel filtration. NPR4 was run over gel filtration with (top) and without (middle) 10 µM SA. NPR4 was also run over gel filtration with [^{3}H]SA and the elution fractions were collected and analyzed for radioactivity (bottom). The peak radioactivity fractions correlate with the NPR4 A_{280} peak and indicates NPR4 binding to SA.

(A)

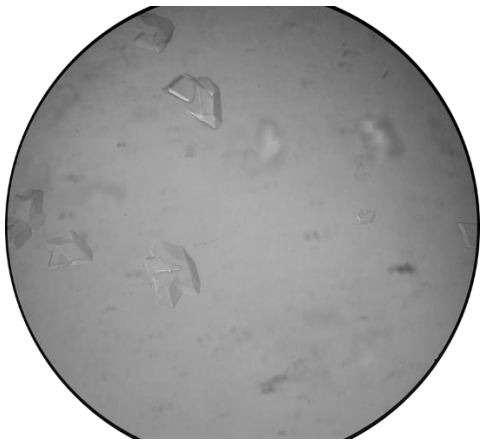

(B)

NPR4 Construct	X-ray diffraction resolution (Å)
Full length (1-574)	10-12
1-552	8-10
1-390	3.2-5

(C)

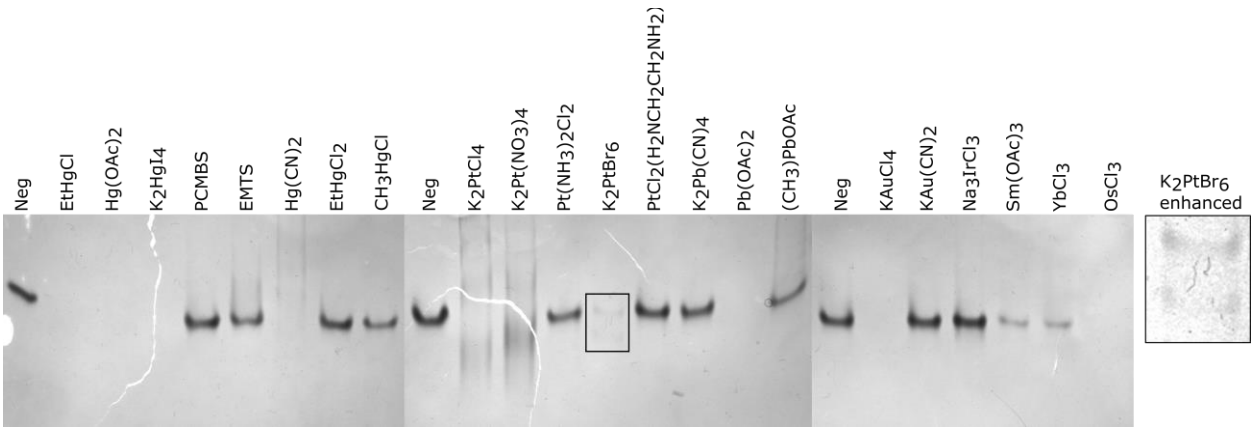

Figure 3.3. NPR4 crystallizes and yields low- to medium-resolution diffraction data. (A) These crystals were grown in 0.1 M Tris pH 7.8, 0.3 M sodium formate, 0.1 M ammonium sulfate, 4% PEG 8000, and 2% poly-γ glutamic acid. They yield X-ray diffraction to a resolution of about 10 Å. **(B)** Further C-terminal NPR4 truncations resulted in increases in resolution, up to 3.2 Å with a 1-390 construct. **(C)** NPR4 1-390 protein (4 μg) was treated with 10 mM of each heavy atom compound for 10 minutes one ice and analyzed on native PAGE. K_2PtBr_6 treatment resulted in a band shift indicative of derivatization (inset).

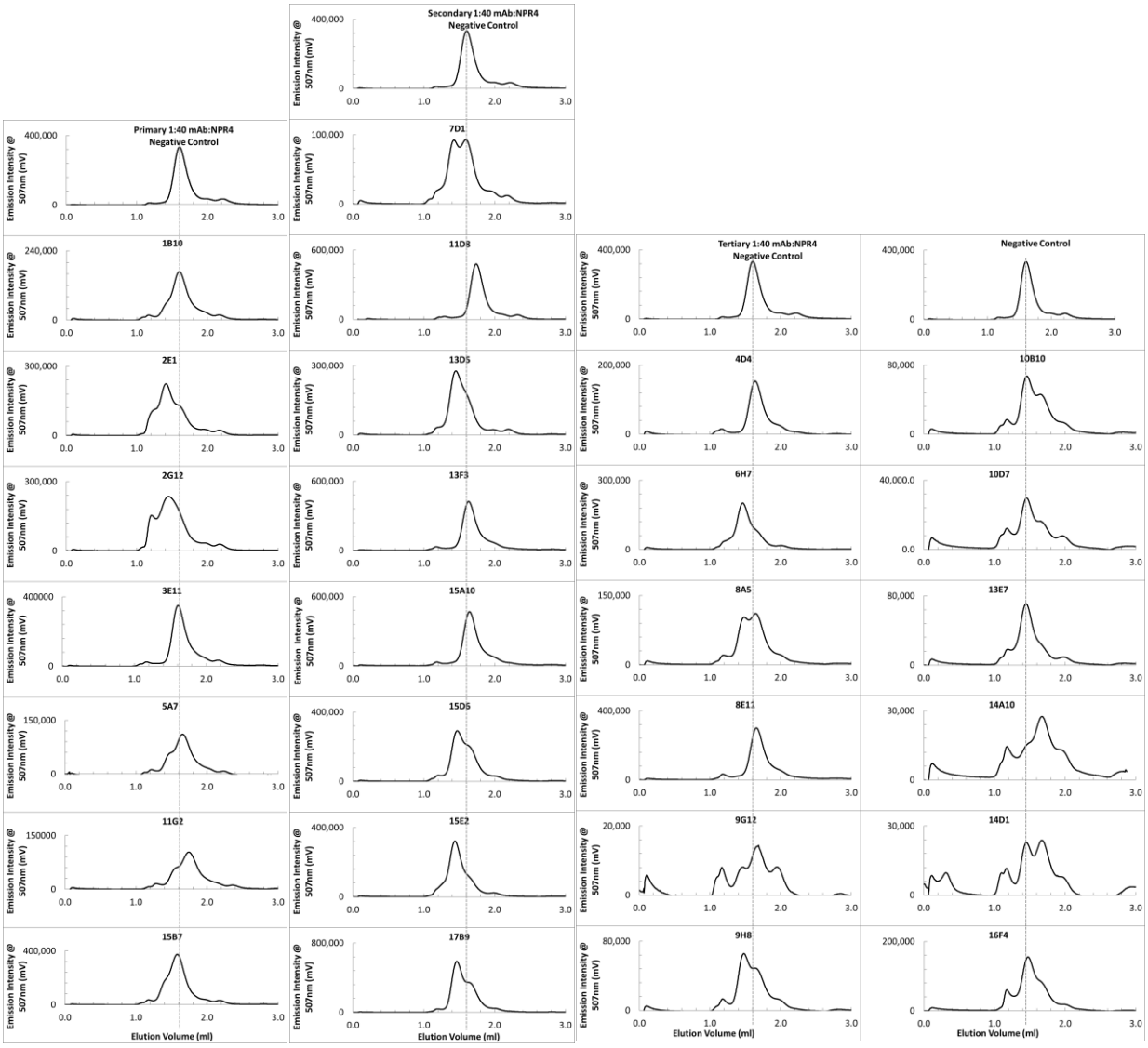

Figure 3.4. NPR4 antibody binding assay. Antibodies generated against NPR4 were separated into three groups (primary, secondary, and tertiary, based on initial data received from manufacturer). Each antibody was mixed with GFP-NPR4 at a 1:40 molar ratio and run over sizing while observing GFP emission at 507 nm. We selected four samples (2G12, 11D8, 13D5, and 15C2) for further analysis based on their ability to shift the GFP emission peak. The gray vertical line indicates GFP emission peak location of the negative control (top).

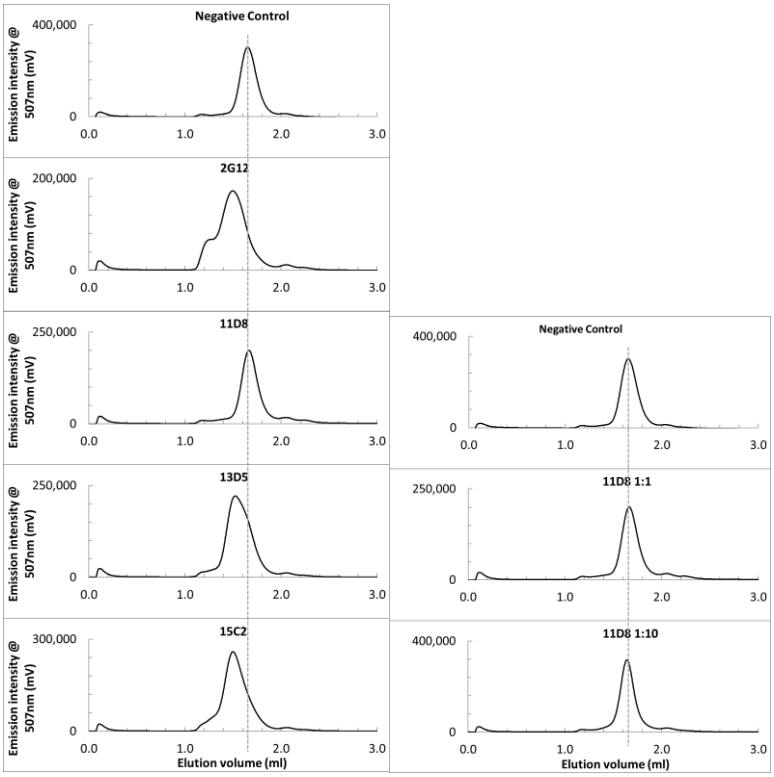

Figure 3.4. NPR4 binds to antibody Fab fragments. Fab fragments were generated from the four selected NPR4 antibodies (2G12, 11D8, 13D5, and 15C2) and run over gel filtration with GFP-NPR4 in a 40:1 ratio (left). All Fab fragments except for 11D8 resulted in a shift in GFP emission at 507 nm. The 11D8 sample was repeated with ratios of 10:1 and 1:1 (right), however no GFP emission peak shifts were observed. The gray vertical line indicates GFP emission peak location of the negative control (top).

BIBLIOGRAPHY

Adams, PD, Afonine, PV, Bunkoczi, G, Chen, VB, Davis, IW, Echols, N, Headd, JJ, Hung, LW, Kapral, GJ, Grosse-Kunstleve, RW, McCoy, AJ, Moriarty, NW, Oeffner, R, Read, RJ, Richardson, DC, Richardson, JS, Terwilliger, TC, and Zwart, PH. 2010. PHENIX: a comprehensive Python-based system for macromolecular structure solution. *Acta Cryst. D* 66: 213-221.

Angers, S, Li, T, MacCoss, MJ, Moon, RT, and Zheng, N. 2006. Molecular architecture and assembly of the DDB1-CUL4A ubiquitin ligase machinery. *Nature* 443: 590-593.

Arias, EE, and Walter, JC. 2006. PCNA functions as a molecular platform to trigger Cdt1 destruction and prevent re-replication. *Nature Cell Biol.* 10.1038-ncb1346.

Bachmair and Varshavsky. 1989. An unstructured initiation site is required for efficient proteasome-mediated degradation. *Cell* 56: 1019-1032.

Benaroudj N, Zwickl P, Seemuller E, Baumeister W, and Goldberg AL. 2003. ATP hydrolysis by the proteasome regulatory complex PAN serves multiple functions in protein degradation. *Mol. Cell* 11: 69–78.

Burroughs, AM, Lakshiminarayan, SB, Iyer, LM, and Aravind, L. 2007. Small but versatile: the extraordinary functional and structural diversity of the β-grasp fold. *Biol. Direct* 2:18 doi: 10.1186/1745-6150-2-18.

Canning, P, Cooper, CDO, Krojer, T, Murray, JW, Pike, ACW, Chaikuad, A, Keates, T, Thangaratnarajah, C, Hojzan, V, Marsden, BD, Gileadi, O, Knapp, S, von Delft, F, and Bullock, AN. 2013. Structural Basis for Cul3 Protein Assembly with the BTB-Kelch Family of E3 Ubiquitin Ligases. *J. Biol. Chem.* 288: 7803-7814.

Cao, H, Bowling, SA, Gordon, AS, and Dong, X. 1994. Characterization of an *Arabidopsis* mutant that is nonresponsive to inducers of systemic acquired resistance. *Plant Cell* 6: 1583-1592.

Cao, H, Glazebrook, J, Clarke, JD, Volko, S, and Dong, X. 1997. The *Arabidopsis* NPR1 gene that controls systemic acquired resistance encodes a novel protein containing ankyrin repeats. *Cell* 88: 57-63.

Cao, H, Li, X, and Dong, X. 1998. Generation of broad-spectrum disease resistance by overexpression of an essential regulatory gene in systemic acquired resistance. *Proc. Nat. Acad. Sci. USA* 95: 6531-6536.

Cardote, TAF, Gadd, MS, and Ciulli, A. 2017. Crystal Structure of the Cul2-Rbx1-EloBC-VHL Ubiquitin Ligase Complex. *Structure* 25: 901-911.

Chamberlain, PP, Lopez-Girona, A, Miller, K, Carmel, G, Pagarigan, B, Chie-Leon, B, Rychak, E, Corral, LG, Ren, YJ, Wang, M, Riley, M, Delker, SL, Ito, T, Ando, H, Mori, T, Hirano, Y, Handa, H, Hakoshima, T, Daniel, TO, and Cathers, BE. 2014. Structure of the human Cereblon–DDB1–lenalidomide complex reveals basis for responsiveness to thalidomide analogs. *Nature Structure & Mol. Biol.* 21: 803-809.

Chamovitz, DA, Wei, N, Osterlund, MT, von Arnim, AG, Staub, JM, Matsui, M, and Deng, XW. 1996. The COP9 complex, a novel multisubunit nuclear regulator involved in light control of a plant developmental switch. *Cell* 86: 115-121.

Chang, L, and Barford, D. 2014. Insights into the anaphase-promoting complex: a molecular machine that regulates mitosis. *Curr. Op. Struct. Biol.* 29: 1-9.

Chau, V, Tobias, JW, Bachmair, A, Marriott, D, Ecker, DJ, Gonda, DK, and Varshavsky, A. 1989. A multiubiquitin chain is confined to specific lysine in a targeted short-lived protein. *Science* 243: 1576-1583.

Cheng, L, Yang, Q, Li, C, Dai, L, Yang, Y, Wang, Q, Ding, Y, Zhang, J, Liu, L, Zhang, S, Fan, P, Hu, X, Xiang, R, Yu, D, Wei, Y, and Deng, H. 2017. DDA1, a novel oncogene, promotes lung cancer progression through regulation of cell cycle. *J. Cell. Mol. Med.* doi:10.1111/jcmm.13084.

Chory, J, Peto, C, Feinbaum, R, Pratt, L, and Ausubel, F. 1989. Arabidopsis thaliana Mutant That Develops as a Light-Grown Plant in the Absence of Light. *Cell* 58: 991-999.

Ciehanover, A, Hod, Y, and Hershko, A. 1978. A heat-stable polypeptide component of an ATP-dependent proteolytic system from reticulocytes. *Biochem. and Biophys. Res. Comm.* 81: 1100-1105.

Cleasby, A, Yon, J, Day, PJ, Richardson, C, Tickle, IJ, Williams, PA, Callahan, JF, Carr, R, Concha, N, Kerns, JK, Qi, H, Sweitzer, T, Ward, P, and Davies, TG. 2014. Structure of the BTB Domain of Keap1 and Its Interaction with the Triterpenoid Antagonist CDDO. *PLoS ONE* 9: e98896.

Desterro, JMP, Rodriguez, MS, Kemp, GD, and Hay, RT. 1999. Identification of the Enzyme Required for Activation of the Small Ubiquitin-like Protein SUMO-1. *J. Biol. Chem.* 274: 10618-10624.

Dias, DC, Dolios, G, Wang, R, and Pan, Z-Q. 2002. CUL7: A DOC domain-containing cullin selectively binds Skp1·Fbx29 to form an SCF-like complex. *Proc. Nat. Acad. Sci. USA* 99: 16601-16606.

Djakbarova, U, Marzluff, WF, and Köseoğlu. 2016. DDB1 and CUL4 associated factor 11 (DCAF11) mediates degradation of Stem-loop binding protein at the end of S phase. *Cell Cycle* 15: 1986-1996.

Duda, DM, Borg, LA, Scott, DC, Hunt, HW, Hammel, M, and Schulman, BA. 2008. Structural Insights into NEDD8 Activation of Cullin-RING Ligases: Conformational Control of Conjugation. *Cell* 134: 995-1006.

Emsley, P, and Cowtan, K. 2004. Coot: model-building tools for molecular graphics. *Acta Cryst. D* 60: 2126-2132.

Finley, D. 2009. Recognition and Processing of Ubiquitin-Protein Conjugates by the Proteasome. *Annu. Rev. Biochem.* 78: 477-513.

Fischer, ES, Scrima, A, Böhm, K, Matsumoto, S, Lingaraju, GM, Faty, M, Yasuda, T, Cavadini, S, Wakasugi, M, Hanaoka, F, Iwai, S, Gut, H, Sugasawa, K, and Thomä, NH. 2011. The Molecular Basis of $CRL4^{DDB2/CSA}$ Ubiquitin Ligase Architecture, Targeting, and Activation. *Cell* 147: 1024-1039.

Fischer, ES, Böhm, K, Lydeard, JR, Yang, H, Stadler, MB, Cavadini, S, Nagel, J, Serluca, F, Acker, V, Lingaraju, GM, Tichkule, RB, Schebesta, M, Forrester, WC, Schirle, M, Hassiepen, U, Ottl, J, Hild, M, Beckwith, REJ, Harper, JW, Jenkins, JL, and Thomä, NH. Structure of the DDB1-CRBN E3 ubiquitin ligase in complex with thalidomide. 2014. *Nature* 512: 49-53.

Fu, ZQ, Yan, S, Saleh, A, Wang, W, Ruble, J, Oka, N, Mohan, R, Spoel, SH, Tada, Y, Zheng, N, and Dong, X. 2012. NPR3 and NPR4 are receptors for the immune signal salicylic acid in plants. *Nature* 486: 228-232.

Furukawa, M, He, YJ, Borchers, C, and Xiong, Y. 2003. Targeting of protein ubiquitination by BTB–Cullin3–Roc1 ubiquitin ligases. *Nat. Cell Biol.* 5: 1001-1007.

Gao, S, Geng, C, Song, T, Lin, X, Liu, J, Cai, Z, and Cang, Y. 2017. Activation of c-Abl Kinase Potentiates the Anti-myeloma Drug Lenalidomide by Promoting DDA1 Protein Recruitment to the CRL4 Ubiquitin Ligase. *J. Biol. Chem.* 292: 3683-3691.

Geng, F, Wenzel, S, Tansey, WP. 2012. Ubiquitin and Proteasomes in Transcription. *Annu. Rev. Biochem.* 81: 177-201.

Goldenberg, SJ, Cascio, TC, Shumway, SD, Garbutt, KC, Liu, J, Xiong, Y, and Zheng, N. 2004. Structure of the Cand1-Cul1-Roc1 Complex Reveals Regulatory Mechanisms for the Assembly of the Multisubunit Cullin-Dependent Ubiquitin Ligases. *Cell* 119: 517-528.

Goldknopf, IL, and Busch, H. 1977. Isopeptide linkage between nonhistone and histone 2A polypeptides of chromosomal conjugate-protein A24. *Proc. Nat. Acad. Sci. USA* 74: 864-868.

Gong, L, Li, B, Millas, S, and Yeh, ETH. 1999. Molecular cloning and characterization of human AOS1 and UBA2, components of the sentrin-activating enzyme complex. *FEBS Letters* 448: 185-189.

Groisman, R, Polanowska, J, Kuraoka, I, Sawada, J-i, Saijo, M, Drapkin, R, Kisselev, AF, Tanaka, K, and Nakatani, Y. 2003. The Ubiquitin Ligase Activity in the DDB2 and CSA Complexes Is Differentially Regulated by the COP9 Signalosome in Response to DNA Damage. *Cell* 113: 357-367.

Gregori, L, Poosch, MS, Cousins, G, and Chau, V. 1990. A Uniform Isopeptide-linked Multiubiquitin Chain Is Sufficient to Target Substrate for Degradation in Ubiquitin-mediated Proteolysis. *J. Biol. Chem.* 265: 8354-8357.

Haas, AL, Bright, PM, and Jackson, VE. 1988. Functional Diversity among Putative E2 Isozymes in the Mechanism of Ubiquitin-Histone Ligation. *J. Biol. Chem.* 263: 13268-13275.

Haas, AL, and Rose, IA. 1982. The mechanism of ubiquitin activating enzyme: A kinetic and equilibrium analysis. *J. Biol. Chem.* 257: 10329-10337.

Haas, AL, Warms, JVB, Hershko, A, and Rose, IA. 1982. Ubiquitin-activating Enzyme: Mechanism and Role in Protein-Ubiquitin Conjugation. *J. Biol. Chem.* 257: 2543-2548.

Havens, CG, and Walter, JC. 2009. Docking of a Specialized PIP Box onto Chromatin-Bound PCNA Creates a Degron for the Ubiquitin Ligase $CRL4^{Cdt2}$. *Mol. Cell* 35: 93-104.

Hershko, A, and Ciechanover, A. 1982. Mechanisms of Intracellular Protein Breakdown. *Annu. Rev. Biochem.* 51: 335-364.

Hershko, A, and Ciechanover, A. 1992. The Ubiquitination System for Protein Degradation. *Annu. Rev. Biochem.* 61: 761-807.

Hershko, A, Ciechanover, A, Heller, H, Haas, AL, and Rose, IA. 1980. Proposed role of ATP in protein breakdown: Conjugation of proteins with multiple chains of the polypeptide of ATP-dependent proteolysis. *Proc. Nat. Acad. Sci. USA* 77: 1783-1786.

Hershko, A, Ciechanover, A, and Rose, IA. 1981. Identification of the Active Amino Acid Residue of the Polypeptide of ATP-dependent Protein Breakdown. *J. Biol. Chem.* 256: 1525-1528.

Hershko, A, and Heller, H. 1985. Occurrence of a polyubiquitin structure in ubiquitin-protein conjugates. *Biochem. and Biophys. Res. Comm.* 128: 1079-1086.

Hershko, A, Heller, H, Elias, S, and Ciechanover, A. 1983. Components of Ubiquitin-Protein Ligase System: Resolution, Affinity Purification, and Role in Protein Breakdown. *J. Biol. Chem.* 258: 8206-8214.

Higa, LAA, Mihaylov, IS, Banks, DP, Zheng, J, and Zhang, H. 2003. Radiation-mediated proteolysis of CDT1 by CUL4–ROC1 and CSN complexes constitutes a new checkpoint. *Nature Cell Biol.* 5: 1008-1015.

Hochstrasser, M. 2009. Origin and function of ubiquitin-like proteins. *Nature* 458: 422-429.

Hori, T, Osaka, F, Chiba, T, Miyamoto, C, Okabayashi, K, Shimbara, N, Kato, S, and Tanaka, K. 1999. Covalent modification of all members of human cullin family proteins by NEDD8. *Oncogene* 18: 6829-6834.

Hu, H, and Sun, S-C. 2016. Ubiquitin signaling in immune responses. *Cell Res.* 26: 457-483.

Huang, W-C, Ko, T-P, Li, SS-L, and Wang, AH-J. 2004. Crystal structures of the human SUMO-2 protein at 1.6 Å and 1.2 Å resolution: Implication on the functional differences of SUMO proteins. *Eur. J. Biochem*. 271: 4114–4122.

Husnjak, K, and Dikic, I. 2012. Ubiquitin-Binding Proteins: Decoders of Ubiquitin-Mediated Cellular Functions. *Annu. Rev. Biochem.* 81: 291-322.

Iovine, B, Iannella, ML, and Bevilacqua, MA. 2011. Damage-specific DNA binding protein 1 (DDB1): a protein with a wide range of functions. *Int. J. of Biochem. and Cell Biol.* 43: 1664-1667.

Irigoyen, ML, Iniesto, E, Rodriguez, L, Puga, MI, Yanagawa, Y, Pick, E, Strickland, E, Paz-Ares, J, Wei, N, De Jaeger, G, Rodriguez, PL, Deng, XW, and Rubio, V. 2014. Targeted Degradation of Abscisic Acid Receptors is Mediated by the Ubiquitin Ligase Substrate Adaptor DDA1 in *Arabidopsis*. *The Plant Cell* 26: 712-728.

Ito, T, Ando, H, Suzuki, T, Ogura, T, Hotta, K, Imamura, Y, Yamaguchi, Y, and Handa, H. 2010. Identification of a Primary Target of Thalidomide Teratogenicity. *Science* 327: 1345-1350.

Jackson, S, and Xiong, Y. 2009. CRL4s: the CUL4-RING E3 ubiquitin ligases. *Trends in Biochem. Sci*. 34: 562-570.

Jin, J, Arias, EE, Chen, J, Harper, JW, and Walter, JC. 2006. A Family of Diverse Cul4-Ddb1-Interacting Proteins Includes Cdt2, which Is Required for S Phase Destruction of the Replication Factor Cdt1. *Mol. Cell* 23: 709-721.

Johnson, ES, Schwienhorst, I, Dohmen, RJ, and Blobel, G. 1997. The ubiquitin-like protein Smt3p is activated for conjugation to other proteins by an Aos1p/Uba2p heterodimer. *EMBO J.* 16: 5509-5519.

Kamura, T, Sato, S, Iwai, K, Czyzyk-Krzeska, M, Conaway, RC, and Conaway, JW. 2000. Activation of HIF1a ubiquitination by a reconstituted von Hippel-Lindau (VHL) tumor suppressor complex. *Proc. Nat. Acad. Sci. USA* 97: 10430-10435.

Kamura, T, Burian, D, Yan, Q, Schmidt, SL, Lane, WS, Querido, E, Branton, PE, Shilatifard, A, Conaway, RC, and Conaway, JW. 2001. MUF1, A Novel Elongin BC-interacting Leucine-rich Repeat Protein That Can Assemble with Cul5 and Rbx1 to Reconstitute a Ubiquitin Ligase. *J. Biol. Chem.* 276: 29748-29753.

Kang, M-Y, Kwon, H-Y, Kim, N-Y, Sakuraba, Y, and Paek, N-C. 2015. *CONSTITUTIVE PHOTOMORPHOGENIC 10* (*COP10*) Contributes to Floral Repression under Non-Inductive Short Days in *Arabidopsis*. *Int. J. of Mol. Sci.* 16: 26493-26505.

Kinkema, M, Fan, W, and Dong, X. 2000. Nuclear localization of NPR1 is required for activation of PR gene expression. *Plant Cell* 12: 2339-2350.

Komander, D, and Rape, M. 2012. The Ubiquitin Code. *Annu. Rev. Biochem.* 81: 203-229.

Koseoglu, MM, Graves, LM, and Marzluff, WF. 2008. Phosphorylation of threonine 61 by cyclin a/Cdk1 triggers degradation of stem-loop binding protein at the end of S phase. *Mol. Cell Biol.* 28: 4469-4479.

Koseoglu, MM, Graves, LM, and Marzluff, WF. 2010. Cyclin A/Cdk1 and CK2 cooperate to trigger degradation of the Stem-loop binding protein (SLBP) at the end of S phase inhibiting histone mRNA biosynthesis. *Febs. J.* 277: 143.

Lechner, E, Leonhardt, N, Eisler, H, Parmentier, Y, Alioua, M, Jacquet, H, Leung, J, and Genschik, P. 2011. MATH/BTB CRL3 receptors target the homeodomain-leucine zipper ATHB6 to modulate abscisic acid signaling. *Dev. Cell* 21: 1116-1128.

Lee, J, and Zhou, P. 2012. Pathogenic role of the CRL4 ubiquitin ligase in human disease. *Frontiers in Oncol*. 2:21 doi:10.3389/fonc.2012.00021.

Li, L, Chai, Q-Y, and Liu, CH. 2016. The ubiquitin system: a critical regulator of innate immunity and pathogen–host interactions. *Cell. & Mol. Immunol.* 13: 560-576.

Li, T, Chen, X, Garbutt, KC, Zhou, P, and Zheng, N. 2006. Structure of DDB1 in Complex with a Paramyxovirus V Protein: Viral Hijack of a Propeller Cluster in Ubiquitin Ligase. *Cell* 124: 105-117.

Liu, C-W, Li, X, Thompson, D, Wooding, K, Chang, T-l, Tang, Z, Yu, H, Thomas, PJ, and DeMartino, GN. 2006. ATP Binding and ATP Hydrolysis Play Distinct Roles in the Function of 26S Proteasome. *Mol. Cell* 24: 39–50.

Liu, J, Furukawa, M, Matsumoto, T, and Xiong, Y. 2002. NEDD8 Modification of CUL1 Dissociates $p120^{CAND1}$, an Inhibitor of CUL1-SKP1 Binding and SCF Ligases. *Mol. Cell* 10: 1511-1518.

Liu, J, Li, T, and Liu, X-L. 2017. DDA1 is induced by NR2F6 in ovarian cancer and predicts poor survival outcome. *Eur. Rev. Med. Pharma.* Sci. 21: 1206-1213.

Lyapina, SA, Correll, CC, Kipreos, ET, and Deshaies, RJ. 1998. Human CUL1 forms an evolutionarily conserved ubiquitin ligase complex (SCF) with SKP1 and an F-box protein. *Proc. Nat. Acad. Sci. USA* 95: 7451-7456.

Ma, L, Zhao, H, and Deng, XW. 2003. Analysis of the mutational effects of the *COP/DET/FUS* loci on genome expression profiles reveals their overlapping yet not identical roles in regulating *Arabidopsis* seedling development. *Dev.* 130: 969-981.

Magesh, S, Chen, Y, and Hu, L. 2012. Small molecule modulators of Keap1-Nrf2-ARE pathway as potential preventative and therapeutic agents. *Med. Res. Rev.* 32: 687-726.

McCall, CM, Miliani de Marval, PL, Chastain II, PD, Jackson, SC, He, YJ, Kotake, Y, Cook, JG, and Xiong, Y. 2008. Human Immunodeficiency Virus Type 1 Vpr-Binding Protein VprBP, a WD40 Protein Associated with the DDB1-CUL4 E3 Ubiquitin Ligase, Is Essential for DNA Replication and Embryonic Development. *Mol. and Cell. Biol.* 28: 5621-5633.

Miura, T, Klaus, W, Gsell, B, Miyamoto, C, and Senn, H. 1999. Characterization of the Binding Interface between Ubiquitin and Class I Human Ubiquitin-conjugating Enzyme 2b by Multidimensional Heteronuclear NMR Spectroscopy in Solution. *J. Mol. Biol.* 290: 213-228.

Moldovan, G-L, Pfander, B, and Jentsch, S. 2007. PCNA, the Maestro of the Replication Fork. *Cell* 129: 665-679.

Mou, Z, Fan, W, and Dong, X. 2003. Inducers of plant systemic acquired resistance regulate NPR1 function through redox changes. *Cell* 113: 935-944.

Muller, S, Matunis, MJ, and Dejean, A. 1998. Conjugation with the ubiquitin-related modifier SUMO-1 regulates the partitioning of PML within the nucleus. *EMBO J.* 17: 61–70.

Muniz, JRC, Guo, K, Kershaw, NJ, Ayinampudi, V, von Delft, F, Babon, JJ, and Bullock, AN. 2013. Molecular Architecture of the Ankyrin SOCS Box Family of Cul5-Dependent E3 Ubiquitin Ligases. *J. Mol. Biol.* 425: 3166-3177.

Murzin, AG. 1992. Structural principles for the propeller assembly of β-sheets: The preference for seven-fold symmetry. *Proteins* 14: 191-201.

Mustilli, AC, Fenzi, F, Ciliento, R, Alfano, F, and Bowler, C. 1999. Phenotype of the Tomato *high-pigment-2* Mutant is Caused by a Mutation in the Tomato Homolog of *DETIOLATED1*. *The Plant Cell* 11: 145-157.

Nijman, SMB, Luna-Vargas, MPA, Velds, A, Brummelkamp, TR, Dirac, AMG, Sixma, TK, and Bernards, R. 2005. A Genomic and Functional Inventory of Deubiquitinating Enzymes. *Cell* 123: 773-786.

Nguyen, T, Yang, CS, and Pickett, CB. 2004. The pathways and molecular mechanisms regulating Nrf2 activation in response to chemical stress. *Free Radic. Biol. Med.* 37: 433-441.

Olma, MH, Roy, M, Bihan, TL, Sumara, I, Maerki, S, Larsen, B, Quadroni, M, Peter, M, Tyers, M, and Pintard, L. 2009. An interaction network of the mammalian COP9 signalosome identifies Dda1 as a core subunit of multiple Cul4-based E3 ligases. *J. Cell Sci.* 122: 1035-1044.

Otwinowski, Z, and Minor, W. 1997. Processing of X-ray Diffraction Data Collected in Oscillation Mode. *Methods in Enzymology* 276: 307-326.

Peters, JL, Schreuder, MEL, Verduin, SJW, and Kendrick, RE. 1992. Physiological characterization of a high-pigment mutant of tomato. *Photochem. Photobiol*. 56:75-82.

Pick, E, Lau, O-S, Tsuge, T, Menon, S, Tong, Y, Dohmae, N, Plafker, SM, Deng, XW, and Wei, N. 2007. Mammalian DET1 Regulates Cul4A Activity and Forms Stable Complexes with E2 Ubiquitin-Conjugating Enzymes. *Mol. and Cell. Biol.* 27: 4708-4719.

Pickart, CM. 2001. Mechanisms Underlying Ubiquitination. *Annu. Rev. Biochem.* 70: 503-533.

Pintard, L, Willems, A, and Peter, M. 2004. Cullin-based ubiquitin ligases: Cul3-BTB complexes join the family. *EMBO J.* 23: 1681-1687.

Prakash, S, Tian, L, Ratliff, KS, Lehotzky, RE, and Matouschek, A. 2004. An unstructured initiation site is required for efficient proteasome-mediated degradation. *Nature Struct. & Mol. Biol.* 9: 830-837.

Rabut, G, Le Dez, G, Verma, R, Makhnevych, T, Knebel, A, Kurz, T, Boone, C, Deshaies, RJ, and Peter, M. 2011. The TFIIH Subunit Tfb3 Regulates Cullin Neddylation. *Mol. Cell* 43: 488-495.

Rachakanda, G, Xiong, Y, Sekhar, KR, Stamer, SL, Liebler, DC, and Freeman, ML. 2008. Covalent modification at Cys151 dissociates the electrophile sensor Keap1 from the ubiquitin ligase Cul3. *Chem. Res. Toxicol.* 21: 705-710.

Rattray, AMJ, and Müller, B. 2012. The control of histone gene expression. *Biochem. Soc. Trans.* 40: 880-885.

Rehman, SAA, Kristariyanto, YA, Choi, S-Y, Nkosi, PJ, Weidlich, S, Labib, K, Hofmann, K, and Kulathu, Y. 2016. MINDY-1 Is a Member of an Evolutionarily Conserved and Structurally Distinct New Family of Deubiquitinating Enzymes. *Mol. Cell* 63: 146-155.

Reynard, GB. 1956. Origin of Webb Special (Black Queen) in tomato. *Rep. Tomato Genet. Coop.* 6: 22.

Ross, AF. Systemic acquired resistance induced by localized virus infections in plants. 1961. *Virology* 14: 340-358.

Rubin, DM, Glickman, MH, Larsen, CN, Dhruvakumar, S, and Finley, D. 1998. Active site mutants in the six regulatory particle ATPases reveal multiple roles for ATP in the proteasome. *EMBO J*. 17: 4909–4919.

Salsman, J, Jagannathan, M, Paladino, P, Chan, P-K, Dellaire, G, Raught, B, and Frappler, L. 2012. Proteomic Profiling of the Human Cytomegalovirus UL35 Gene Products Reveals a Role for UL35 in the DNA Repair Response. *J. Virol.* 86: 806-820.

Sang, Y, Yan, F, and Ren, X. 2015. The role and mechanism of CRL4 E3 ubiquitin ligase in cancer and its potential therapy implications. *Oncotarget* 6: 42590-42602.

Schlesinger, DH, Goldstein, G, and Niall, HD. 1975. The Complete Amino Acid Sequence of Ubiquitin, an Adenylate Cyclase Stimulating Polypeptide Probably Universal in Living Cells. *Biochem.* 14: 2214-2218.

Schroeder, DF, Gahrtz, M, Maxwell, BB, Cook, RK, Kan, JM, Alonso, JM, Ecker, JR, and Chory, J. 2002. De-Etiolated 1 and Damaged DNA Binding Protein 1 Interact to Regulate Arabidopsis Photomorphogenesis. *Curr. Biol.* 12: 1462-1472.

Scrima, A, Fischer, ES, Lingaraju, GM, Böhm, K, Cavadini, S, and Thomä, NH. 2011. Detecting UV-lesions in the genome: The modular CRL4 ubiquitin ligase does it best! *FEBS Letters* 585: 2818-2825.

Scrima, A, Koníčková, Czyzewski, BK, Kawasaki, Y, Jeffrey, PD, Groisman, R, Nakatani, Y, Iwai, S, Pavletich, NP, and Thomä, NH. 2009. Structural Basis of UV DNA-Damage Recognition by the DDB1-DDB2 Complex. *Cell* 135: 1213-1223.

Scott, DC, Sviderskiy, VO, Monda, JK, Lydeard, JR, Cho, SE, Harper, JW, and Schulman, BA. 2014. Structure of a RING E3 Trapped in Action Reveals Ligation Mechanism for the Ubiquitin-like Protein NEDD8. *Cell* 157: 1671-1684.

Sheard, LB, Tan, X, Mao, H, Withers, J, Ben-Nissan, G, Hinds, TR, Kobayashi, Y, Hsu, F-F, Sharon, M, Browse, J, He, SY, Rizo, J, Howe, GA, and Zheng, N. 2010. Jasmonate perception by inositol-phosphate-potentiated COI1-JAZ co-receptor. *Nature* 468: 400-405.

Sivakumar, S, and Gorbsky, GJ. 2015. Spatiotemporal regulation of the anaphase-promoting complex in mitosis. *Nat. Rev. Mol. Cell Biol.* 16: 82-94.

Smith, DM, Kafri, G, Cheng, Y, Ng, D, Walz, T, and Goldberg, AL. 2005. ATP Binding to PAN or the 26S ATPases Causes Association with the 20S Proteasome, Gate Opening, and Translocation of Unfolded Proteins. *Mol. Cell* 20: 687-698.

Soressi, GP. 1975. New spontaneous or chemically induced fruit ripening tomato mutants. *Rep. Tomato Genet. Coop.* 25: 21-22.

Spoel, SH, Mou, Z, Tada, Y, Spivey, NW, Genschik, P, and Dong, X. 2009. Proteasome-mediated turnover of the transcriptional coactivator NPR1 plays dual roles in regulating plant immunity. *Cell* 137: 860-872.

Srivastava, S, Swanson, SK, Manel, N, Florens, L, Washburn, MP, Skowronski, J. 2008. Lentiviral Vpx Accessory Factor Targets VprBP/DCAF1 Substrate Adaptor for Cullin 4 E3 Ubiquitin Ligase to Enable Macrophage Infection. *PLoS Pathog.* 4: e1000059.

Tan, X, Calderon-Villalobos, LIA, Sharon, M, Zheng, C, Robinson, CV, Estelle, M, and Zheng, N. 2007. Mechanism of auxin perception by the TIR1 ubiquitin ligase. *Nature* 446: 640-645.

Tong, KI, Padmanabhan, B, Kobayashi, A, Shang, C, Hirotsu, Y, Yokoyama, S, and Yamamoto, M. 2007. Different Electrostatic Potentials Define ETGE and DLG Motifs as Hinge and Latch in Oxidative Stress Response. *Mol. and Cell Biol.* 27: 7511-7521.

Uknes, S, Mauch-Mani, B, Moyer, M, Potter, S, Williams, S, Dincher, S, Chandler, D, Slusarenko, A, Ward, E, and Ryals, J. 1992. Acquired resistance in *Arabidopsis*. *Plant Cell* 4: 645-656.

van der Veen, AG, and Ploegh, HL. 2012. Ubiquitin-Like Proteins. *Annu. Rev. Biochem.* 81: 323-357.

van Tuinen, A, Cordonnier-Pratt, MM, Pratt, LH, Verkerk, R, Zabel, P, and Koornneef, M. 1997. The mapping of phytochrome genes and photomorphogenic mutants of tomato. *Theor. Appl. Genet.* 94: 115-122.

van Wijk, SJL, and Timmers, HTM. 2010. The family of ubiquitin-conjugating enzymes (E2): deciding between life and death of proteins. *FASEB J.* 24: 981-993.

Verma, R, Aravind, L, Oania, R, McDonald, WH, Yates III, JR, Koonin, EV, Deshaies, RJ. 2002. Role of Rpn11 Metalloprotease in Deubiquitination and Degradation by the 26S Proteasome. *Science* 298: 611-615.

Vijay-Kumar, S, Bugg, CE, Wilkinson, KD, and Cook, WJ. 1985. Three-dimensional structure of ubiquitin at 2.8 Å resolution. *Proc. Nat. Acad. Sci. USA* 82: 3582-3585.

Vijay-Kumar, S, Bugg, CE, and Cook, WJ. 1987. Structure of Ubiquitin Refined at 1.43 Å Resolution. *J. Mol. Bio*. 194: 531-544.

Wang, D, Weaver, ND, Kesarwani, M, and Dong, X. 2005. Induction of protein secretory pathway is required for systemic acquired resistance. *Science* 308: 1036-1040.

Wang, D, Amornsiripanitch, N, and Dong, X. 2006. A genomic approach to identify regulatory nodes in the transcriptional network of systemic acquired resistance in plants. *PLoS Pathog.* 2: e123.

Wilkinson, KD, and Audhya, TK. 1981. Stimulation of ATP-dependent proteolysis requires ubiquitin with the COOH-terminal sequence Arg-Gly-Gly. *J. Biol. Chem.* 256: 9235-9241.

Wu, Y, Zhang, D, Chu, JY, Boyle, P, Wang, Y, Brindle, ID, De Luca, V, and Deprés, C. 2012. The *Arabidopsis* NPR1 protein is a receptor for the plant defense hormone salicylic acid. *Cell Rep.* 28: 639-647.

Wu, Y, Zhou, X, Barnes, CO, DeLucia, M, Cohen, AE, Gronenborn, AM, Ahn, J, and Calero, G. 2016. The DDB1–DCAF1–Vpr–UNG2 crystal structure reveals how HIV-1 Vpr steers human UNG2 toward destruction. *Nature Struct. and Mol. Biol.* 23: 933-940.

Yanagawa, Y, Sullivan, JA, Komatsu, S, Gusmaroli, G, Suzuki, G, Yin, J, Ishibashi, T, Saijo, Y, Rubio, V, Kimura, S, Wang, J, and Deng, XW. 2004. *Arabidopsis* COP10 forms a complex with DDB1 and DET1 in vivo and enhances the activity of ubiquitin conjugating enzymes. *Genes and Dev.* 18: 2172-2181.

Yen, HC, Shelton, BA, Howard, LR, Lee, S, Vrebalov, J, and Giovannoni, JJ. 1997. The tomato *high-pigment* (*hp*) locus maps to chromosome 2 and influences plastome copy number and fruit quality. *Theor. Appl. Genet.* 95: 1069-1079.

Zhang, Y, Fan, W, Kinkema, M, Li, X, and Dong, X. 1999. Interaction of NPR1 with basic leucine zipper protein transcription factors that bind sequences required for salicylic acid induction of the PR-1 gene. *Proc. Natl. Acad. Sci. USA* 96: 6523-6528.

Zhang, Y, Han, D, Yu, P, Huang, Q, and Ge, P. 2017. Genome-scale transcriptional analysis reveals key genes associated with the development of type II diabetes in mice. *Exp. and Therap. Med.* 13: 1044-1050.

Zhao, S, Tang, H, Yan, D, Fan, J, Sun, H, Wen, Y, Yu, F, Cui, F, Zhang, D, Xue, Y, Liu, C, Yue, B, Chen, J, Wang, J, Wang, X, Zhang, M, Yu, Y, Jiang, W, Liu, X, Mi, Y, Zhou, Z, Qin, X, and Peng, Z. 2016. DDA1 promotes stage IIB–IIC colon cancer progression by activating NFκB/CSN2/GSK-3β signaling. *Oncotarget* 7: 19794-19812.

Zheng, N, Schulman, BA, Song, L, Miller, JJ, Jeffrey, PD, Wang, P, Chu, C, Koepp, DM, Elledge, SJ, Pagano, M, Conaway, RC, Conaway, JW, Harper, JW, and Pavletich, NP. 2002. Structure of the Cul1–Rbx1–Skp1–Fbox^{Skp2} SCF ubiquitin ligase complex. *Nature* 416: 703-709.

Zheng, N, and Shabek, N. 2017. Ubiquitin Ligases: Structure, Function, and Regulation. *Annu. Rev. Biochem.* 86: 14.1-14.29.

VITA

Jim Ruble grew up in Grandville, MI. After graduation from Grandville High School in 2000 he enlisted in the U.S. Navy. He was assigned to the VQ-1 "World Watchers" and served as an avionics technician and electronic warfare operator aboard EP-3E reconnaissance aircraft. Jim's service spanned two wars and multiple operations around the world. In 2005, he completed his active duty service and subsequently began his academic career. He earned a B.S. in Cell and Molecular Biology in 2010 with minors in Chemistry and Psychology from Grand Valley State University in Allendale, MI while conducting research into the structural basis of antibiotic resistance. He was admitted to the doctoral program in the Department of Pharmacology at the University of Washington School of Medicine and successfully defended his thesis in 2017. In his spare time Jim enjoys strength training and hiking in Washington's Cascade mountains, and is an avid follower of geopolitics.